Report 3308

NAVAL SHIP RESEARCH AND DEVELOPMENT CENTER

Washington, D.C. 20007

[redacted]

INTEGRAL METHODS FOR TURBULENT BOUNDARY LAYERS IN PRESSURE GRADIENTS

by

Paul S. Granville

DEPARTMENT OF HYDROMECHANICS
RESEARCH AND DEVELOPMENT REPORT

April 1970

Report 3308

INTEGRAL METHODS FOR TURBULENT BOUNDARY LAYERS IN PRESSURE GRADIENTS

The Naval Ship Research and Development Center is a U.S. Navy center for laboratory effort directed at achieving improved sea and air vehicles. It was formed in March 1967 by merging the David Taylor Model Basin at Carderock, Maryland and the Marine Engineering Laboratory (now Naval Ship R & D Laboratory) at Annapolis, Maryland. The Mine Defense Laboratory (now Naval Ship R & D Laboratory) Panama City, Florida became part of the Center in November 1967.

Naval Ship Research and Development Center
Washington, D.C. 20007

MAJOR NSRDC ORGANIZATIONAL COMPONENTS

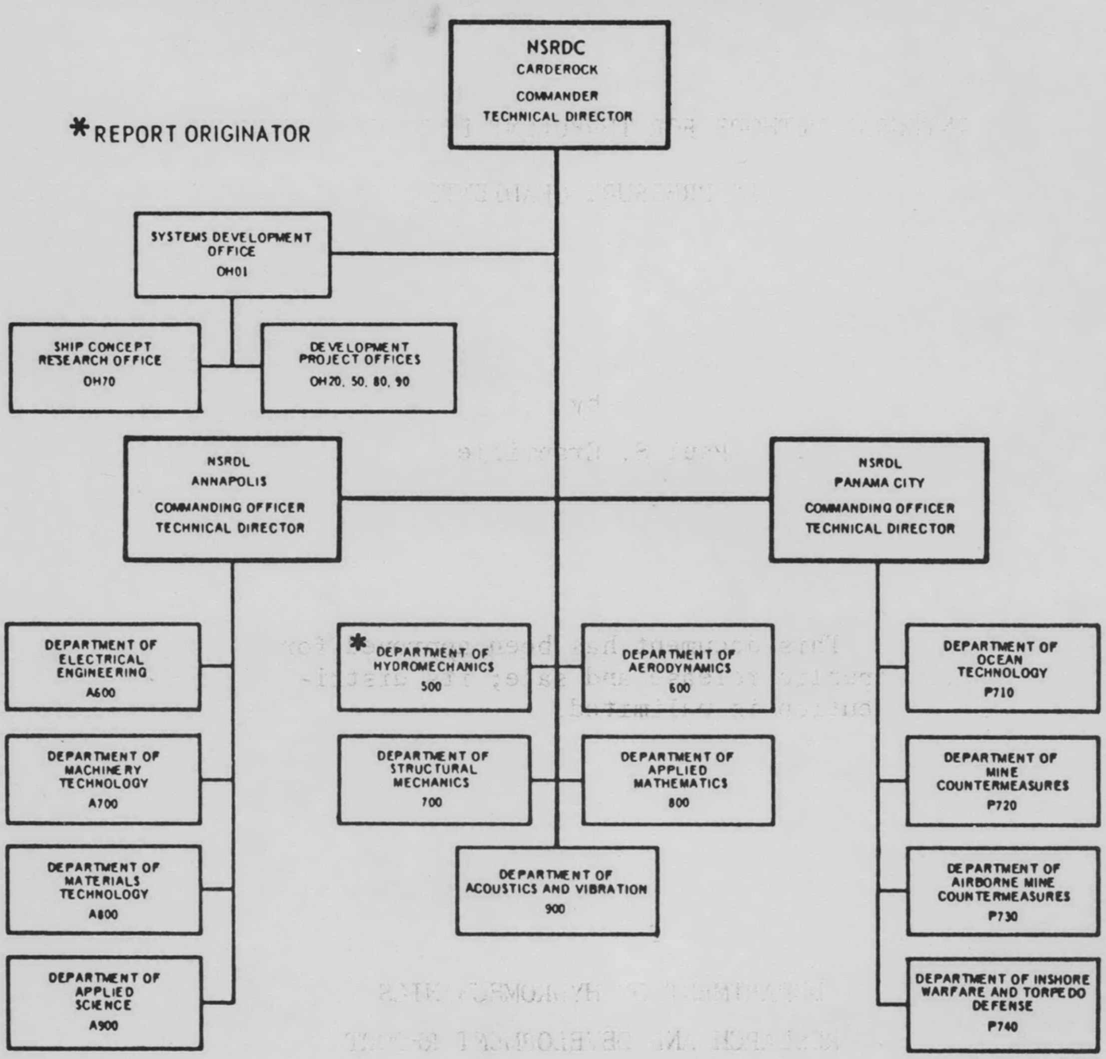

NDW-NSRDC 3960/43 (10-67)

DEPARTMENT OF THE NAVY
NAVAL SHIP RESEARCH AND DEVELOPMENT CENTER
WASHINGTON, D. C. 20007

INTEGRAL METHODS FOR TURBULENT BOUNDARY LAYERS IN PRESSURE GRADIENTS

by

Paul S. Granville

April 1970 Report 3308

TABLE OF CONTENTS

LIST OF FIGURES

NOTATION

A	Slope of logarithmic velocity law
$\mathcal{A}$	Factor in equation for flat-plate shape parameter, Equation (42)
B_1, B_2	Intercepts of logarithmic velocity laws, Equations (6) and (9)
$\mathcal{B}$	Factor in equation for flat-plate shape parameter, Equation (42)
C_D	Dissipation integral defined in Equation (89)
$\hat{C}_D$	Dissipation integral defined in Equation (94)
C_S	General shear-stress factor given in Equation (82)
$\hat{C}_S$	General shear-stress factor defined in Equation (84)
C_τ	Shear-stress integral defined in Equation (192)
c_1, c_2	Constants in Equation (26)
c_3, c_4	Constants in Equation (35)
E	Entrainment factor, Equation (115)
e	Subscript denoting equilibrium conditions
G	Rotta's shape parameter defined in Equation (21)
G^*	Velocity-defect energy shape parameter defined in Equation (54)
$\hat{G}$	Velocity-defect shape parameter defined in Equation (169)
$\bar{G}$	Velocity-defect shape parameter defined in Equation (172)
H	Shape parameter, $H = \delta^*/\theta$
H^*	Energy shape parameter defined in Equation (45)
$\tilde{H}$	Entrainment shape parameter defined in Equation (60)
$\hat{H}$	Shape parameter defined in Equation (140)
$\bar{H}$	Shape parameter defined in Equation (141)
I_1	Velocity-defect integral defined in Equation (32)
M	Pressure-gradient coefficient, Equation (82)
m	Relative position in boundary layer, $m = s/\delta$
N	Coefficient in Equation (82)
n	Power-law exponent, Equation (16)
P	Coefficient in Equation (82)
p	Pressure

R_θ	Momentum-thickness Reynolds number, $R_\theta = U\theta/\nu$
s	y-position in boundary layer
U	Velocity at outer edge of boundary layer
u	Mean tangential velocity component in boundary layer
u'	Fluctuating tangential velocity
u_s	u at position y = s
u_τ	Shear velocity, $u_\tau = \sqrt{\tau_w/\rho}$
u_*	General shear velocity, $u_* = \sqrt{\tau^*/\rho}$
v	Mean normal velocity component
v'	Fluctuating normal velocity
w	Coles' wake factor
x	Streamwise distance
y	Normal distance from wall
o	Subscript denoting flat-plate conditions
0.3	Subscript denoting conditions at m = 0.3
α_1, α_2	Constants in Equation (28)
β	Clauser's pressure-gradient parameter defined in Equation (70)
γ	Velocity ratio, $(u/U)_{y=\theta}$, Equation (25)
δ	Boundary-layer thickness
δ^*	Displacement thickness
ζ	Factor in Equation (114)
θ	Momentum thickness
θ^*	Energy thickness defined in Equation (44)
λ	Constant in Equation (202)
ν	Kinematic viscosity
ρ	Density
τ	Shear stress in boundary layer
τ_s	τ at y = s
τ_w	Wall shear stress
τ^*	Characteristic shear stress, Equation (3)
ψ_o	Factor in Equation (201)

ABSTRACT

Shape parameter differential equations are developed for turbulent boundary layers in pressure gradients incorporating two-parameter velocity profiles. Energy and entrainment methods are included. Shear stress factors are explicitly developed for equilibrium and quasi-equilibrium conditions.

ADMINISTRATIVE INFORMATION

This work was funded by the Naval Ordnance Systems Command under Subproject UR 109 01 03.

INTRODUCTION

The analytical prediction of turbulent boundary layers in pressure gradients has been the subject of intensive investigation not only because of the engineering applications but also because of the difficulties in developing methods suitable for all types of pressure distributions. The fundamental problem of the turbulent boundary layer is common to that of all turbulent flow: the lack of an adequate theory on the mechanics of turbulent motion.

Rotta[1-3] has critically examined the various predictive methods which have appeared in the literature in recent years. The 1968 Stanford Conference[4] tested the ability of current methods to predict existing experimental results from given pressure distributions.

Among the trends which may be ascertained from the Stanford Conference are:

1. The virtual abandonment of traditional θ-H formulations (θ = momentum thickness, H = shape parameter) when utilizing two-parameter velocity profiles such as the Coles law of the wake. However results are still given in terms of θ and H.

2. The use of shear stress factors, (e.g., the dissipation integral for the energy equation) derived from equilibrium pressure gradients for use in non-equilibrium pressure gradients.

---

[1]References are listed on page 43.

It is now proposed to return to the traditional θ-H methods even for two-parameter velocity profiles in deriving shape parameter equations for the various integral methods. Analytical relations are obtained for the various shape parameters for two-parameter velocity profiles. Analytical expressions are also derived for the various shear-stress factors under equilibrium pressure gradients. Consideration is given to applying equilibrium shear-stress factors to non-equilibrium pressure gradients.

VELOCITY SIMILARITY LAWS FOR BOUNDARY LAYER FLOW WITH PRESSURE GRADIENTS

The velocity similarity laws, the law of the wall and the velocity defect law, provide an analytical basis for pipe flow and boundary layer flow on flat plates (in zero pressure gradient). The extension to boundary-layer flow with pressure gradients may be made to proceed as follows:

INNER LAW OR LAW OF THE WALL

In addition to pressure gradient dp/dx, the mean velocity component u parallel to the smooth wall (roughness and other effects may also be included) is considered to be dependent on the usual local quantities: normal distance from the wall y, shearing stress at the wall τ_w, density ρ and kinematic viscosity ν of the fluid or

$$u = f\left[\tau_w, \ \rho, \ \nu, y, \ \frac{dp}{dx}\right] \tag{1}$$

Non-dimensional ratios may be formed

$$\frac{u}{u_\tau} = f\left[\frac{u_\tau \, y}{\nu}, \ \frac{\nu}{\rho \, u_\tau^3}\frac{dp}{dx}\right] \tag{2}$$

where $u_\tau = \sqrt{\tau_w/\rho}$, shear velocity.

OUTER LAW OR VELOCITY DEFECT LAW

In the boundary layer away from the wall, the velocity defect U - u at a relative position in the boundary y/δ develops as a consequence of the cumulative effect of the pressure gradients which may be represented by some appropriate characteristic value of the shearing stress τ^*. Mickley et al.[5] uses the value of shearing stress τ at the inner edge of the outer layer as τ^*; for adverse pressure gradients τ^* becomes the maximum value of τ and for zero pressure gradient τ_w. Likewise McDonald and Stoddart[6] use the maximum value of τ as τ^* for adverse pressure gradients. The density ρ is an additional physical parameter. Analytically then

$$U - u = f[y/\delta, \rho, \tau^*] \tag{3}$$

where δ is boundary layer thickness and U is value of u at $y = \delta$. Non-dimensionally

$$\frac{U-u}{u_*} = F\left[\frac{y}{\delta}\right] \tag{4}$$

where u_* is $\sqrt{\tau^*/\rho}$.

For flat plates (zero pressure gradient) $\tau^* \to \tau_w$ and $u_{\tau^*} \to u_\tau$.

LOGARITHMIC LAW

Within the boundary layer the ranges of validity of the inner and outer laws are considered to overlap which results in logarithmic functions for both the inner and outer laws for the common region. Equating the derivatives of u with respect to y for the inner and outer laws, Equations (2) and (4), produces

$$\left(\frac{u_\tau y}{\nu}\right) \frac{\partial\left(u/u_\tau\right)}{\partial(u_\tau\ y/\nu)} = -\frac{u_*}{u_\tau}\left(\frac{y}{\delta}\right)\frac{\partial\left(\frac{U-u}{u_*}\right)}{\partial(y/\delta)} = A \tag{5}$$

Then integrating

$$\frac{u}{u_\tau} = A\ \ell n\ \frac{u_\tau y}{\nu} + B_1\left[\frac{\nu}{\rho\ u_\tau^3}\frac{dp}{dx}\right] \tag{6}$$

Experimentally Patel[7] shows $B_1 = B_{1,0}$ for $\left(\nu/\rho u_\tau^{\ 3}\right)$ (dp/dx) < 0.01 where $B_{1,0} = B_1[0]$ for flat plates (zero pressure gradient).

Also

$$\frac{U-u}{u_\tau^*} = - \frac{u_\tau}{u_\tau^*} A \ln \frac{y}{\delta} + B_{2,0} \tag{7}$$

or

$$\frac{U-u}{u_\tau} = - A \ln \frac{y}{\delta} + \frac{u_{\tau^*}}{u_\tau} B_{2,0} \tag{8}$$

or

$$\frac{U-u}{u_\tau} = - A \ln \frac{y}{\delta} + B_2 \tag{9}$$

where $B_2 = \left(u_\tau^*/u_\tau\right) B_{2,0}$ and $B_{2,0} = B_2$ for flat plates (zero pressure gradient).

The value of B_2 then depends on the history of the effects of the pressure gradients up to the station being considered or $B_2 = f[x]$. For specially adjusted pressure gradients termed equilibrium pressure gradients, B_2 can be held constant with respect to x. Boundary layers on flat plates in zero pressure gradient may be considered as a special case of equilibrium boundary layers with $B_2 = B_{2,0}$. In general even for equilibrium pressure gradients $B_2 \neq B_{2,0}$. Towards separation $B_2 \to \infty$.

LAW OF THE WAKE

It was observed by Coles[8] that the experimental data for the outer law outside the overlapping region had similarity in its deviation from the logarithmic law such that

$$\frac{U-u}{u_\tau} = - A \ln \frac{y}{\delta} + B_2 \left(1 - \frac{1}{2} w \left[\frac{y}{\delta}\right]\right) \tag{10}$$

where $w[y/\delta]$ is considered as a universal function termed the wake function. The wake function given in tabular form by Coles[8] was fitted with a sigmoidal function by Hinze[9]

$$w = 1 + \sin\left[\frac{y}{\delta} \pi - \frac{\pi}{2}\right] = 1 - \cos\left[\frac{y}{\delta} \pi\right] \tag{11}$$

A polynomial fit is given by Moses[10] as

$$w = 2\left[3\left(\frac{y}{\delta}\right)^2 - 2\left(\frac{y}{\delta}\right)^3\right] \tag{12}$$

In an earlier analysis Rotta[11] used as a first approximation a linear function

$$w = 2\,\frac{y}{\delta} \tag{13}$$

The wake function is normalized so $\int_0^1 w\,d[y/\delta] = 1$. Also $w[1] = 2$.

BOUNDARY LAYER PARAMETERS

GENERAL

Analytical models of the velocity profile are designated one-parameter if

$$\frac{u}{U} = f\left[\frac{y}{\theta}\,,\ H\right] \tag{14}$$

and two-parameter if

$$\frac{u}{U} = f\left[\frac{y}{\theta}\,,\ H,\ R_\theta\right] \tag{15}$$

where θ, momentum thickness = $\int_0^\delta (1 - u/U)\ (u/U)\,dy$;

δ^*, displacement thickness = $\int_0^\delta (1 - u/U)\,dy$;

H, shape parameter (due to Gruschwitz) = δ^*/θ; and

R_θ, momentum thickness Reynolds number = $U\theta/\nu$.

POWER LAW

An example of a one-parameter velocity profile is the familiar power law

$$\frac{u}{U} = \left(\frac{y}{\delta}\right)^n \tag{16}$$

which produces

$$H = 2\,n + 1 \tag{17}$$

$$\frac{\delta^*}{\delta} = \frac{H - 1}{H + 1} \tag{18}$$

$$\frac{\theta}{\delta} = \frac{H - 1}{H(H+1)} \tag{19}$$

Then

$$\frac{u}{U} = \left[\left(\frac{y}{\theta}\right)\frac{(H - 1)}{H(H+1)}\right]^{\frac{H-1}{2}} \tag{20}$$

As shown in Figure 5 of Reference 12 the power law model provides a surprisingly close fit to experimental velocity profiles in pressure gradients.

VELOCITY SIMILARITY LAWS

The velocity similarity laws provide a two-parameter velocity profile.

A useful shape parameter is Rotta's shape parameter (also called Clauser's shape parameter)

$$G \equiv \frac{\int_o^1 \left(\frac{U-u}{u_\tau}\right)^2 d\left(\frac{y}{\delta}\right)}{\int_o^1 \left(\frac{U-u}{u_\tau}\right) d\left(\frac{y}{\delta}\right)} \tag{21}$$

If the velocity defect law is assumed to hold also to the wall, G is constant for constant B_2 of equilibrium boundary layers. Also from the definitions

$$G = \frac{U}{u_\tau}\left(\frac{H-1}{H}\right) = \left(\frac{\tau_w}{\rho\ U^2}\right)^{-\frac{1}{2}}\left(\frac{H-1}{H}\right) \tag{22}$$

From the law of the wake

$$G = \frac{4\ A^2 + 3.18\ A\ B_2 + 0.75\ B_2{}^2}{2\ A + B_2} \tag{23}$$

WALL SHEARING STRESS

The coefficient of wall shearing stress or local skin friction is expressed by

$$\frac{\tau_w}{\rho\ U^2} = f\left[H,\ R_\theta\right] \tag{24}$$

As shown by Rotta[1] and Patel,[13] the law of the wake provides an implicit relationship for $\left(\tau_w/\rho U^2\right)\left[H, R_\theta\right]$. However an explicit relationship obtained in Reference 12 is a generalization of the procedure of Ludwieg and Tillmann[14] or

$$\frac{\tau_w}{\rho\ U^2} = \left(\frac{\tau_w}{\rho\ U^2}\right)_o \left(\frac{\gamma}{\gamma_o}\right)^{\frac{4}{H_o+1}} \tag{25}$$

where $\left(\tau_w/\rho U^2\right)_o$ is the flat plate value for the same R_θ, $\left(\tau_w/\rho U^2\right)_o = f\left[R_\theta\right]$. $\gamma = (u/U)_{y=\theta}$, γ_o, and H_o are the flat plate values.

Empirically both Uram[15] and Felsch[16] express γ as

$$\gamma = c_1 - c_2 \log H \tag{26}$$

(Here log is taken as $\log_{10}$.)
Uram gives $c_1 = 0.9058$ and $c_2 = 1.818$ while Felsch gives $c_1 = 0.93$ and $c_2 = 1.95$.

At separation, $\tau_w/\rho U^2 = 0$, Uram's constants give H = 3.15 and Felsch's constants give H = 3 which is closer to test data than H = 4 given by the law of the wake. Nash[17] uses H = 3 at separation in a modified skin-friction formula for pressure gradients. Also Equation (25) with Felsch's constants for γ gives a very close fit to Nash's recommendation.

WALL SHEARING STRESS FOR FLAT PLATES

As shown in Reference 12, $\left(\tau_w/\rho U^2\right)_o\left[R_\theta\right]$ is derived from the Schoenherr formula for the total drag of flat plates as

$$\left(\frac{\tau_w}{\rho\ U^2}\right)_o = \frac{0.0146}{\left(\log\left[2\ R_\theta\right]\right)\left(1/2\ \log\ \left[2\ R_\theta\right]\ +\ 0.4343\right)} \tag{27}$$

Formulas of type

$$\left(\frac{\tau_w}{\rho\ U^2}\right)_o = \frac{1}{\left(\alpha_1\ R_\theta\ +\ \alpha_2\right)^2} \tag{28}$$

may also be derived as follows:

Adding the overlapping inner and outer logarithmic laws, Equations (6) and (9) produces

$$\frac{U}{u_\tau} = A\ \ell n\ \frac{u_\tau\ \delta}{\nu} + B_1 + B_2 \tag{29}$$

Since $u_\tau \delta/\nu = (u_\tau/U)\ (\delta/\theta)\ R_\theta$ by definition

$$\frac{U}{u_\tau} = -\ A\ \ell n\ \frac{U}{u_\tau} + A\ \ell n\ R_\theta\ -\ A\ \ell n\ \frac{\theta}{\delta} + B_1 + B_2 \tag{30}$$

If the velocity defect law is assumed to hold to the wall

$$\frac{\theta}{\delta} = \frac{u_\tau}{U}\ I_1 \left(1\ -\ \frac{u_\tau}{U}\ G\right) = \frac{u_\tau}{U}\ \frac{I_1}{H} \tag{31}$$

where

$$I_1 \equiv \int_0^1 \left(\frac{U-u}{u_\tau}\right) d\left(\frac{y}{\delta}\right) \tag{32}$$

From the law of the wake

$$I_1 = A + \frac{1}{2} B_2 \tag{33}$$

Then for flat plates denoted by subscript o

$$\frac{U}{u_\tau} = A \ell n\ R_\theta + A \ell n\ H_o - A \ell n\ I_{1,0} + B_1 + B_{2,0} \tag{34}$$

If

$$\ell n\ H_o \cong c_3 + c_4 \frac{U}{u_\tau} \tag{35}$$

then

$$\frac{U}{u_\tau} = \alpha_1 \log R_\theta + \alpha_2 \tag{36}$$

or

$$\left(\frac{\tau_w}{\rho U^2}\right)_o = \frac{1}{\left(\alpha_1 \log R_\theta + \alpha_2\right)^2} \tag{37}$$

where

$$\alpha_1 = \frac{2.3026\ A}{1-c_4\ A} \tag{38}$$

and

$$\alpha_2 = \frac{B_1 + B_{2,0} + c_3\ A - \ell n\left(A + 1/2\ B_{2,0}\right)}{1-c_4\ A}$$

SHAPE PARAMETER FOR FLAT PLATES

Since from Equation (22)

$$\frac{H_o}{H_o - 1} = \frac{1}{G_o \sqrt{\left(\frac{\tau_w}{\rho U^2}\right)_o}} \tag{40}$$

then from Equation (37)

$$\frac{H_o}{H_o - 1} = \frac{\alpha_1}{G_o} \log R_\theta + \frac{\alpha_2}{G_o} \tag{41}$$

or

$$\frac{H_o}{H_o - 1} = \mathcal{A} \log R_\theta + \mathcal{B} \tag{42}$$

or

$$H_o = \left[1 - \left(\mathcal{A} \log R_\theta + \mathcal{B}\right)^{-1}\right]^{-1} \tag{43}$$

where $\mathcal{A} = \frac{\alpha_1}{G_o}$ and $\mathcal{B} = \frac{\alpha_2}{G_o}$

ENERGY THICKNESS AND SHAPE PARAMETER

The energy thickness θ^* is defined as

$$\theta^* \equiv \int_0^\delta \frac{u}{U}\left[1 - \left(\frac{u}{U}\right)^2\right]dy \tag{44}$$

The energy shape parameter H^* is defined as

$$H^* \equiv \theta^*/\theta \tag{45}$$

For one-parameter velocity profiles

$$H^* = f\,[H] \tag{46}$$

while for two-parameter velocity profiles

$$H^* = f\left[H,\ R_\theta\right] \tag{47}$$

The simplest relation is from the power-law velocity profile, a one-parameter velocity profile, which is

$$H^* = \frac{4H}{3H-1} = \frac{\frac{4}{3}H}{H - \frac{1}{3}} \tag{48}$$

Closer empirical fits (one-parameter) have been obtained by various investigators.[18-22]

From Weighardt:

$$H^* = \frac{1.269\ H}{H - 0.379} \qquad 1.25 < H < 1.7 \tag{49}$$

From Fernholz:

$$H^* = \frac{1.272\ H}{H - 0.37} + 5.4\left(\frac{H}{10}\right)^4 \qquad \begin{array}{c} 1.35 < H < 2.8 \\ 5 \times 10^3 < R_\theta < 2.5 \times 10^4 \end{array} \tag{50}$$

From Moses et al.:

$$H^* = \frac{1.02 + 0.87\ H + 0.095\ H^2}{H} \tag{51}$$

From Goldberg:

$$H^* = \frac{3.6\ H}{2.78\ H - 1} \tag{52}$$

From Nicoll and Escudier:

$$H^* = 1.431 - \frac{0.0971}{H} + \frac{0.775}{H^2} \qquad \begin{array}{c} 1.25 < H < 2.8 \\ 10^3 < R_\theta < 8 \times 10^4 \end{array} \tag{53}$$

A two-parameter relation $H^* = f\left[H, R_\theta\right]$ may be obtained from the velocity similarity laws as follows. A velocity-defect law energy shape parameter G^* is defined as follows

$$G^* \equiv \frac{\int_o^1 \left(\frac{U-u}{u_\tau}\right)^3 d\left(\frac{y}{\delta}\right)}{\int_o^1 \left(\frac{U-u}{u_\tau}\right) d\left(\frac{y}{\delta}\right)} \tag{54}$$

From the appropriate definitions

$$H^* = \frac{\left(\frac{u_\tau}{U}\right)^2 G^* - 3\left(\frac{u_\tau}{U}\right) G + 2}{1 - \left(\frac{u_\tau}{U}\right) G} \tag{55}$$

Then, from Equation (22)

$$H^* = 3 - H + \left(\frac{G^*}{G^2}\right)\frac{(H-1)^2}{H} \qquad (56)$$

Equation (56) was also obtained by Rotta.[11]

From the law of the wake

$$G^* = \frac{12\ A^3 + 11.04\ A^2\ B_2 + 4.71\ A\ B_2^{\ 2} + 0.63\ B_2^{\ 3}}{2\ A + B_2} \qquad (57)$$

G^* and G are then related through Equations (57) and (23) with B_2 being the implicit parameter. At separation $B_2 \to \infty$ and $G^*/G^2 \to 1.12$. An explicit numerical fit gives closely

$$\frac{G^*}{G^2} = 1.12 + \frac{1.5}{G} \qquad (58)$$

Then with Equation (56) and Equation (22)

$$H^* = 3 - H + 1.12\ \frac{(H-1)^2}{H} + 1.5\ (H-1)\sqrt{\frac{\tau_w}{\rho\ U^2}} \qquad (59)$$

where the variation with R_θ is obtained through $\tau_w/\rho U^2$ given by Equation (25).

The comparison in Figure 1 shows excellent agreement between the two-parameter relation and the empirical one-parameter relations of Fernholz and of Nicoll and Escudier.

ENTRAINMENT THICKNESS AND SHAPE PARAMETER

The entrainment thickness is defined as $\delta - \delta^*$ and the entrainment shape parameter $\tilde{H}$ as

$$\tilde{H} \equiv \frac{\delta - \delta^*}{\theta} = \frac{\delta}{\theta} - H \qquad (60)$$

For one-parameter velocity profiles

$$\tilde{H} = f\ [H] \qquad (61)$$

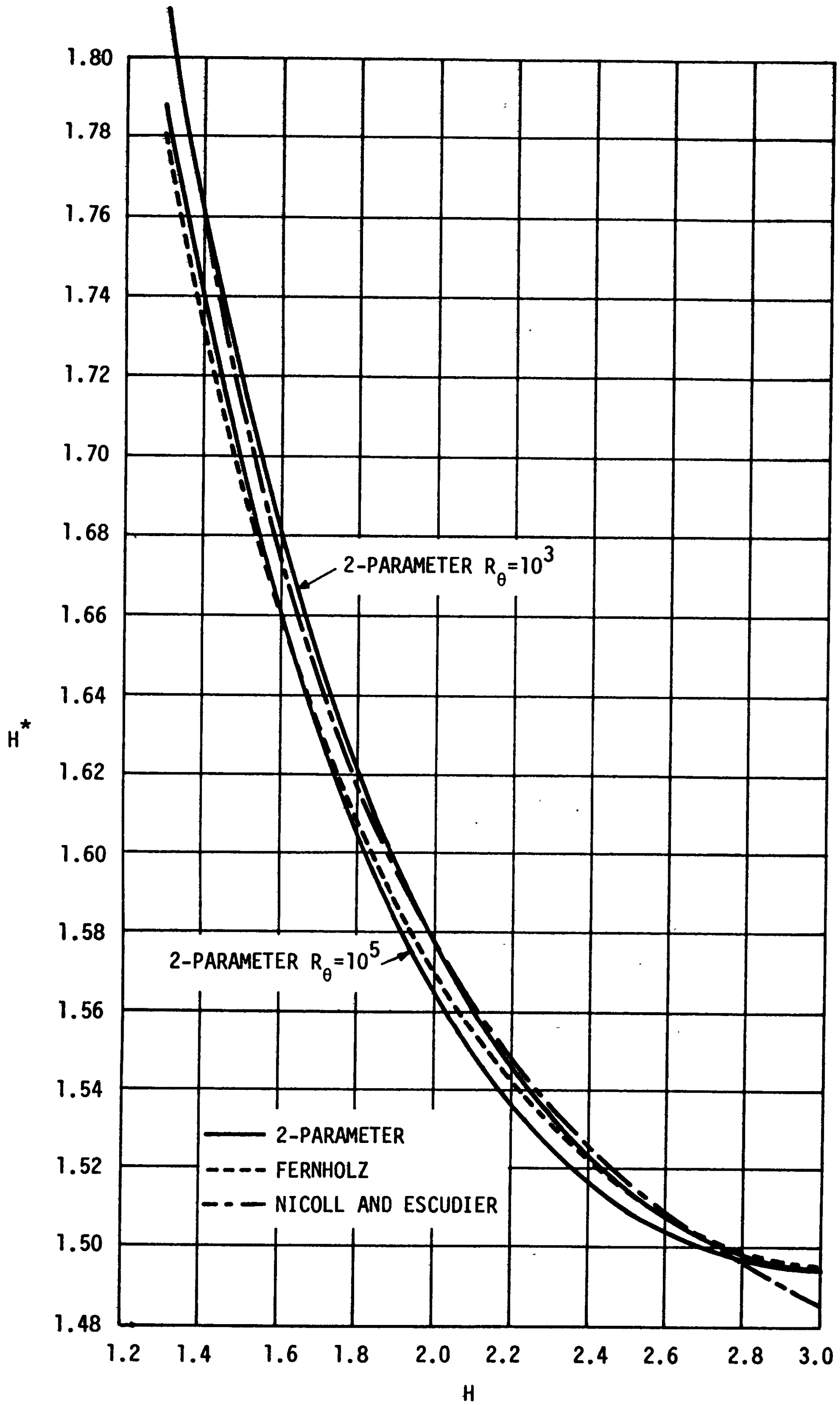

Figure 1 - Comparison of Energy Shape Parameters

while for two-parameter velocity profiles

$$\tilde{H} = f\left[H,\ R_\theta\right] \tag{62}$$

The power law velocity profile gives

$$\tilde{H} = \frac{2H}{H - 1} \tag{63}$$

An empirical fit by Head[4] yields the one-parameter relation

$$\tilde{H} = 1.535\ (H-0.7)^{-2.715} + 3.3 \tag{64}$$

A relation $\tilde{H} = f\left[H, R_\theta\right]$ may be obtained from the velocity similarity laws. From the definition

$$\frac{\theta}{\delta} = \frac{u_\tau}{U} I_1 \left(1 - \frac{u_\tau}{U} G\right) \tag{65}$$

Then from Equation (22)

$$\frac{\theta}{\delta} = \frac{I_1}{G}\left(\frac{H - 1}{H^2}\right) \tag{66}$$

and from Equation (60)

$$\tilde{H} = \left(\frac{G}{I_1}\right)\left(\frac{H^2}{H - 1}\right) - H \tag{67}$$

This relation was also obtained by Michel et al.[4]

I_1 and G may be related through Equations (33) and (23) with B_2 being the implicit parameter. At separation $B_2 \to \infty$ and $G/I_1 \to 1.5$. A close numerical fit gives

$$\frac{G}{I_1} = 1.5 + \frac{3.8}{G^{3/2}} \tag{68}$$

Then from Equation (67)

$$\tilde{H} = \frac{H(H+2)}{2(H-1)} + \frac{3.8\ H^{7/2}}{(H-1)^{5/2}}\left(\frac{\tau_w}{\rho\ U^2}\right)^{\frac{3}{4}} \tag{69}$$

For $H = 3$, $\tau_w/\rho U^2 = 0$ and $\tilde{H} = 3.75$.

The comparison in Figure 2 shows close agreement between the two-parameter values and the empirical fit of Head.

EQUILIBRIUM PRESSURE GRADIENTS

EFFECT OF PRESSURE GRADIENT PARAMETER

It has been shown theoretically by Rotta and experimentally by Clauser that similarity is maintained if the pressure gradient parameter

$$\beta \equiv \frac{\delta^*}{\tau_w}\frac{dp}{dx} \tag{70}$$

is kept constant with respect to x or $d\beta/dx = 0$.

Then G and consequently B_2 are constant. Empirically Nash[23] obtains

$$G = 6.1\sqrt{1.81 + \beta} - 1.7 \tag{71}$$

Felsch[16] obtains

$$G = 6\sqrt{1.8 + \beta} - 1.5 \tag{72}$$

and Alber[4,24]

$$\begin{aligned} G &= 6.1\sqrt{1.81 + \beta} - 0.40, \quad && \beta \geq 0 \\ G &= 6.5\,\beta + 7.8067, && \beta < 0 \end{aligned} \tag{73}$$

SHAPE PARAMETER

For equilibrium pressure gradients Equation (34) is stated as

$$\frac{U}{u_\tau} = A \ln R_\theta + A \ln H - A \ln I_1 + B_1 + B_2 \tag{74}$$

From Equation (22)

$$\frac{H}{H-1} = \frac{1}{G}\frac{U}{u_\tau} = \frac{A}{G}\ln R_\theta + \frac{A}{G}\ln H - \frac{A}{G}\ln I_1 + \frac{B_1}{G} + \frac{B_2}{G} \tag{75}$$

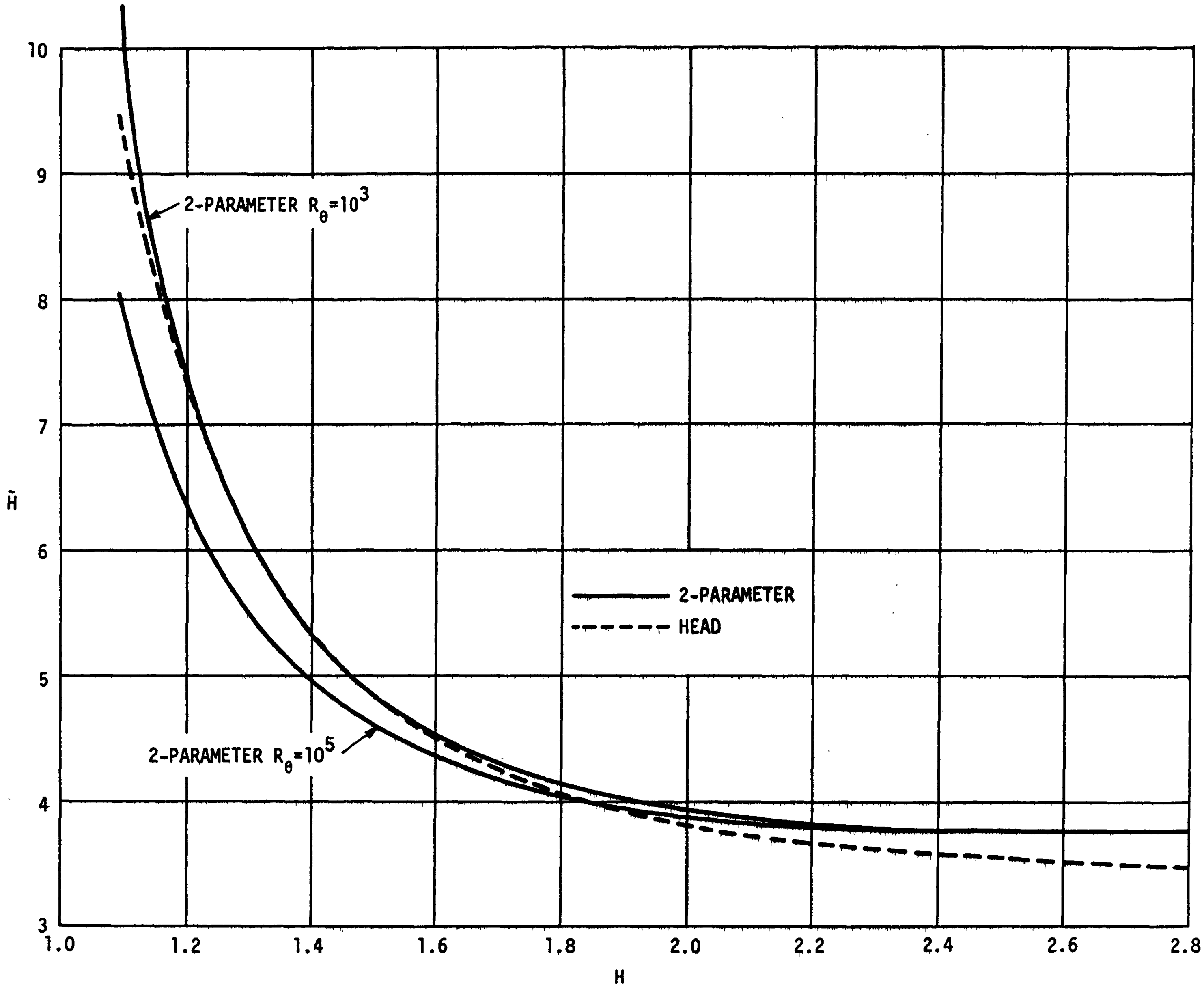

Figure 2 - Comparison of Entrainment Shape Parameters

In general A is constant and B_1 is constant for smooth surfaces. For equilibrium boundary layers G, I_1 and B_2 are constant with respect to x for a particular β.

Differentiating Equation (75) with respect to x produces

$$\theta \frac{dH}{dx} = - \frac{A(H-1)^2 \left[H+(H+1)\beta\right] \frac{\tau_w}{\rho \; U^2}}{G \; H + A(H-1)^2} \tag{76}$$

for equilibrium boundary layers.

An alternate form from Equation (22) is

$$\theta \frac{dH}{dx} = - \frac{G \; H \frac{\partial}{\partial \; \ell n \; R_\theta} \left(\frac{\tau_w}{\rho \; U^2}\right)^{\frac{1}{2}} \left[H + (H+1)\beta\right] \frac{\tau_w}{\rho \; U^2}}{G \; H^2 \frac{\partial}{\partial H} \left(\frac{\tau_w}{\rho \, U^2}\right)^{\frac{1}{2}} - 1} \tag{77}$$

where $\tau_w / \rho U^2$ is given by Equation (25).

INTEGRAL METHODS

GENERAL

Integral methods for solving the turbulent boundary layers in pressure gradients refer to methods based on integrated forms of the equation of motion (momentum equation) and/or the equation of continuity, using various weighting factors which for incompressible two-dimensional flow are

$$u \frac{\partial u}{\partial x} + v \frac{\partial u}{\partial y} = U \frac{dU}{dx} + \frac{1}{\rho} \frac{\partial \tau}{\partial y} \tag{78}$$

$$\frac{\partial u}{\partial x} + \frac{\partial x}{\partial y} = 0 \tag{79}$$

The shearing stress τ includes both laminar and turbulent contributions

$$\tau = \mu \frac{du}{dy} - \rho\, \overline{u'v'} \tag{80}$$

where $\overline{u'v'}$ = Reynolds turbulent shear stress. The Reynolds turbulent normal stresses are not included though these may become quite significant close to separation. Also close to separation $\partial p/\partial y \neq 0$.

The classical integral form is von Kármán's momentum equation obtained by integrating the equation of motion without using any weighting factor

$$\frac{d\theta}{dx} + (H+2)\frac{\theta}{U}\frac{dU}{dx} = \frac{\tau_w}{\rho\, U^2} \tag{81}$$

The purpose of other integrated forms is to obtain eventually the variation of H with x or dH/dx. The energy equation uses **u** as a weighting factor. The entrainment equation integrates the equation of continuity. The moment-of-momentum equation uses y as the weighting factor. The partial momentum equations partially integrate the equation of motion to differently specified sublevels within the boundary layer. Details of these equations follow.

The shape parameter equation may take the following forms

$$\theta \frac{dH}{dx} = -M\left[H, R_\theta\right] \frac{\theta}{U}\frac{dU}{dx} + N\left[H, R_\theta\right] \frac{\tau_w}{\rho\, U^2} - P\left[H, R_\theta\right] C_S \tag{82}$$

or

$$\theta \frac{dH}{dx} = -M\left[H, R_\theta\right] \frac{\theta}{U}\frac{dU}{dx} - \left(P\left[H, R_\theta\right] \cdot \hat{C}_S - N\left[H, R_\theta\right]\right) \frac{\tau_w}{\rho\, U^2} \tag{83}$$

where M, N, P are coefficients, C_S is the generalized shear-stress factor and

$$\hat{C}_S = \frac{C_S}{\tau_w/\rho U^2} \tag{84}$$

EQUILIBRIUM SHEAR-STRESS FACTORS

To obtain $C_S\left[H, R_\theta\right]$ for equilibrium boundary layers, $\theta dH/dx$ from Equation (83) is first converted to form

$$\theta \frac{dH}{dx} = \left(\frac{\beta M}{H} - P\,\hat{C}_S + N\right)\frac{\tau_w}{\rho\,U^2} \tag{85}$$

and equated to Equation (76) to produce

$$\hat{C}_{S,e} = \frac{\beta M}{HP} + \frac{N}{P} + \frac{A(H-1)^2\ [H+(H+1)\beta]}{\left[GH + A(H-1)^2\right]P} \tag{86}$$

where $\hat{C}_{S,e}$ represents the equilibrium value of $\hat{C}_S$.

$\hat{C}_{S,e}$ may be considered a function of H and R_θ if β is related to G by Equation (71) and G is a function of H and R_θ through Equation (22).

ENERGY METHOD

GENERAL

The energy equation is obtained by multiplying the equation of motion Equation (78) by u and integrating over the whole boundary layer

$$\frac{d}{dx}\left(U^3\ \theta^*\right) = \frac{2}{\rho}\int_0^\delta \tau\,\frac{\partial u}{\partial y}\,dy \tag{87}$$

In terms of energy shape parameter $H^* \equiv \theta^*/\theta$ and employing the momentum equation for $d\theta/dx$

$$\theta\,\frac{dH^*}{dx} = (H-1)H^*\,\frac{\theta}{U}\,\frac{dU}{dx} - H^*\,\frac{\tau_w}{\rho\,U^2} + C_D \tag{88}$$

where

$$C_D \equiv \frac{2}{\rho\,U^3}\int_0^\delta \tau\,\frac{\partial u}{\partial y}\,dy \tag{89}$$

called the dissipation integral, the shear-stress work integral or the production integral.

SHAPE PARAMETER EQUATION

The objective is to convert the energy shape parameter equation, Equation (88), to a shape parameter equation of forms Equations (82) or (83).

For a two-parameter velocity profile

$$H^* = H^* \left[H, \ln R_\theta\right] \tag{90}$$

Then expanding into partial derivatives

$$\theta \frac{dH^*}{dx} = \frac{\partial H^*}{\partial H} \theta \frac{dH}{dx} + \frac{\partial H^*}{\partial \ln R_\theta} \theta \frac{d \ln R_\theta}{dx} \tag{91}$$

or

$$\theta \frac{dH^*}{dx} = \frac{\partial H^*}{\partial H} \theta \frac{dH}{dx} + \frac{\partial H^*}{\partial \ln R_\theta}\left[\frac{\tau_w}{\rho U^2} - (H+1) \frac{\theta}{U} \frac{dU}{dx}\right] \tag{92}$$

and finally

$$\theta \frac{dH}{dx} = \left[(H-1)H^* + (H+1) \frac{\partial H^*}{\partial \ln R_\theta}\right] \frac{\partial H}{\partial H^*} \frac{\theta}{U} \frac{dU}{dx}$$
$$- \left[H^* + \frac{\partial H^*}{\partial \ln R_\theta} - \hat{C}_D\right] \frac{\partial H}{\partial H^*} \frac{\tau_w}{\rho U^2} \tag{93}$$

where

$$\hat{C}_D \equiv 2 \int_0^1 \frac{\tau}{\tau_w} \frac{\partial (u/U)}{\partial (y/\delta)} d\left(\frac{y}{\delta}\right) \tag{94}$$

Then from Equation (82)

$$M = - \left[(H-1)H^* + (H+1) \frac{\partial H^*}{\partial \ln R_\theta}\right] \frac{\partial H}{\partial H^*} \tag{95}$$

$$N = - \left(H^* + \frac{\partial H^*}{\partial \ln R_\theta}\right) \frac{\partial H}{\partial H^*} \tag{96}$$

and

$$P = -\frac{\partial H}{\partial H^*} \tag{97}$$

$C_{D,e}$ is obtained from Equation (86) since $C_{D,e} = C_{S,e}$ for the energy equation.

POWER-LAW ENERGY THICKNESS

Here

$$H^* = f[H] = \frac{4H}{3H-1} \tag{48}$$

Then

$$\frac{dH^*}{dH} = -\frac{4}{(3H-1)^2} \tag{98}$$

$$M = H(H-1)\ (3H-1) \tag{99}$$

$$N = H(3H-1) \tag{100}$$

$$P = \frac{1}{4}\ (3H-1)^2 \tag{101}$$

and

$$\hat{C}_{D,e} = \frac{4[(H-1)\beta+H]}{3H-1} + \frac{4\ A(H-1)^2\ [H+(H+1)\beta]}{(3H-1)^2\left[GH + A(H-1)^2\right]} \tag{102}$$

FERNHOLZ ENERGY THICKNESS

Here

$$H^* = \frac{1.272\ H}{H - 0.37} + 5.4 \times 10^{-4}\ H^4 \tag{50}$$

Then

$$\frac{dH^*}{dH} = -\frac{0.4706}{(H-0.37)^2} + 2.16 \times 10^{-3}\ H^3 \tag{103}$$

$$M = \frac{(H-1)(H-0.37)\left[1.272\ H + 5.4 \times 10^{-4}\ (H-0.37)H^4\right]}{0.4706 - 2.16 \times 10^{-3}\ (H-0.37)^2\ H^3} \tag{104}$$

$$N = \frac{M}{H-1} \tag{105}$$

$$P = -\frac{dH}{dH^*} = \frac{(H-0.37)^2}{0.4706 - 2.16 \times 10^{-3} \ (H-0.37)^2 \ H^3} \tag{106}$$

and

$$\hat{C}_{D,e} = \left[\frac{(H-1)}{H} \ \beta + 1\right] H^* - \left\{\frac{A(H-1)^2 \left[H + (H+1)\beta\right]}{GH + A(H-1)^2}\right\} \frac{dH^*}{dH} \tag{107}$$

TWO-PARAMETER ENERGY THICKNESS

Here

$$H^* = 3 - H + \frac{1.12(H-1)^2}{H} + 1.5 \ (H-1) \sqrt{\frac{\tau_w}{\rho \ U^2}} \tag{59}$$

With Equation (25)

$$\frac{\partial H^*}{\partial H} = -1 + \frac{1.12\left(H^2-1\right)}{H^2} + 1.5\sqrt{\frac{\tau_w}{\rho \ U^2}} \left[1 - \frac{2 \ c_2 \ (H-1)}{2.3\left(H_o+1\right) \ H\gamma}\right] \tag{108}$$

and with Equations (37) and (42)

$$\frac{\partial H^*}{\partial \ \ell n \ R_\theta} = -1.5(H-1) \sqrt{\frac{\tau_w}{\rho \ U^2}} \left[\frac{\alpha_1}{2.3}\left(\frac{\tau_w}{\rho \ U^2}\right)_o^{\frac{1}{2}} + \frac{2\mathcal{a}(H_o-1)^2}{2.3(H_o+1)}\left(\frac{c_2}{2.3 \ H_o\gamma_o} - \frac{\ell n \ \frac{\gamma}{\gamma_o}}{H_o+1}\right)\right] \tag{109}$$

M, N, P, and $C_{D,e}$ are obtained from Equations (95), (96), (97), and (86).

Figure 3 shows how close the M values are for the various formulations.

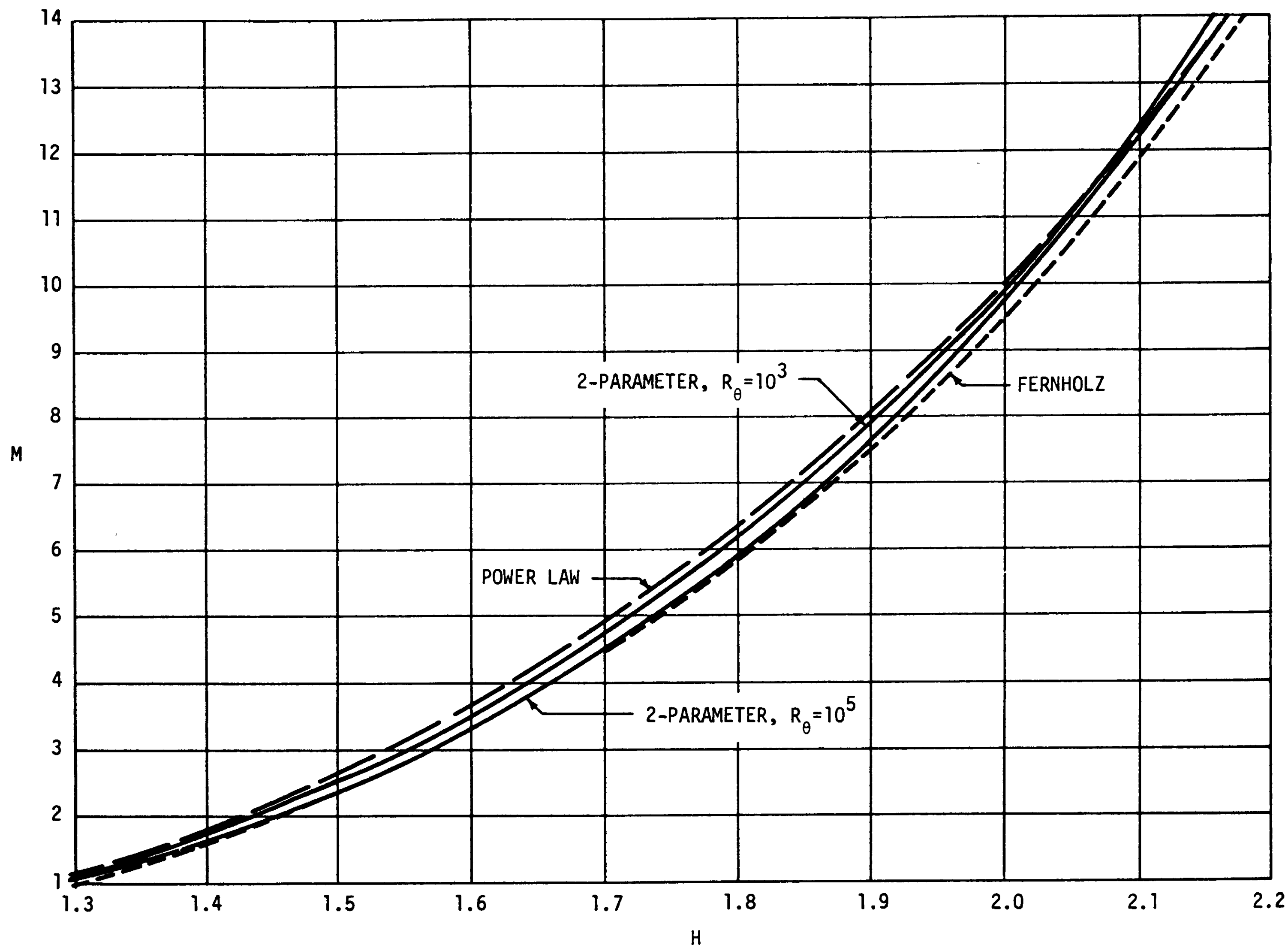

Figure 3 - Energy Method, $M = f[H, R_\theta]$; Comparison of Various Procedures

EXISTING RELATIONS FOR DISSIPATION INTEGRAL

Truckenbrodt[25] approximates

$$C_D = \frac{0.0112}{R_\theta^{1/6}} \tag{110}$$

from the analyses of Rotta.[11]

Walz[26] suggests for equilibrium boundary layers

$$C_{D,e} = \frac{0.00962 + 0.1644\ (H^* - 1.5)^{4.81}}{R_\theta^{(0.2317H - 0.2644)}} \tag{111}$$

where H^* is determined by Fernholz, Equation (50).

A fit of experimental shear-stress data by Escudier and Spalding[27] results in

$$C_D = 1.094\ \frac{\tau_w}{\rho\ U^2} + 0.004214\ H - 0.004572 \tag{112}$$

Escudier et al.[28] propose

$$C_D = \frac{2}{3}\ (2\ \zeta + 1)\ \frac{\tau_w}{\rho\ U^2} + 0.0113\ (1 - \zeta)^{2.715} \tag{113}$$

where

$$\zeta = \frac{2}{3} H^* - 1 + \sqrt{\frac{2}{3} H^* \left(\frac{2}{3} H^* - 1\right)} \tag{114}$$

Figure 4 compares the dissipation integral for the various formulations.

ENTRAINMENT METHOD

GENERAL

The entrainment equation was first proposed by Head[29,4] on the basis of physical reasoning regarding the growth or entrainment of the developing boundary layer. It has since been found out that it can be derived by integrating the equation of continuity, Equation (79). Michel et al.[4]

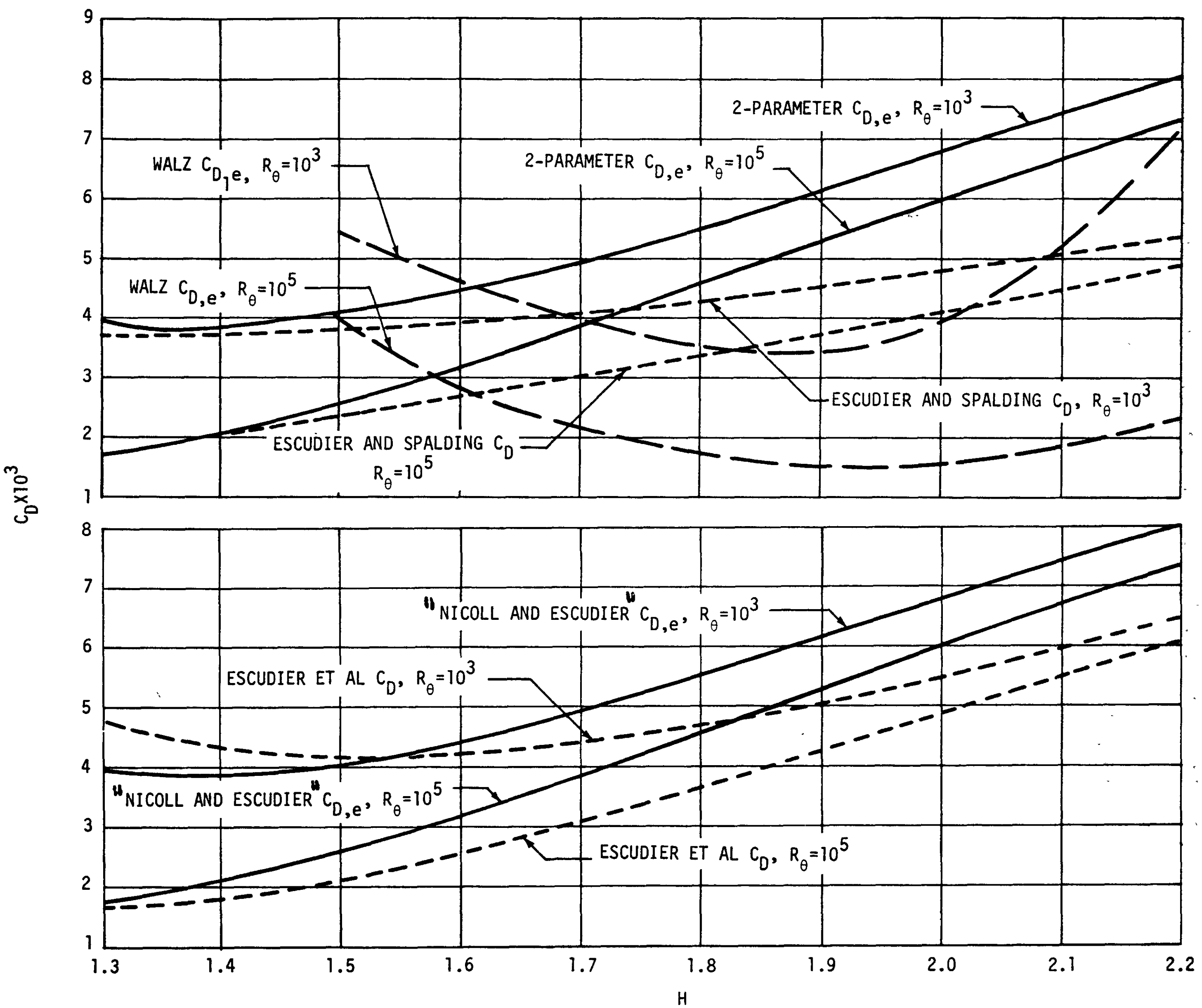

Figure 4 - Energy Method, $C_D = f[H, R_\theta]$; Comparison of Various Procedures

introduced a shear-stress factor by considering the equation of motion Equation (78) at $y = \delta$. The entrainment equation then resembles the energy equation and is given by

$$\frac{1}{U}\frac{d}{dx}\left[U(\delta-\delta^*)\right] = -\frac{1}{\rho U}\left(\frac{\partial\tau}{\partial u}\right)_\delta = E \tag{115}$$

In terms of the entrainment shape parameter $H = (\delta - \delta^*)/\theta$ and employing the momentum equation for $d\theta/dx$

$$\theta\frac{d\tilde{H}}{dx} = (\tilde{H}+1)H\frac{\theta}{U}\frac{dU}{dx} - \tilde{H}\frac{\tau_w}{\rho U^2} + E \tag{116}$$

SHAPE PARAMETER EQUATION

The objective is to convert the entrainment shape parameter equation, Equation (116), to a shape parameter equation of forms Equations (82) or (83).

For a two-parameter velocity profile

$$\tilde{H} = f\left[H,\ \ell n\ R_\theta\right] \tag{117}$$

Then expanding into partial derivatives

$$\theta\frac{d\tilde{H}}{dx} = \frac{\partial\tilde{H}}{\partial H}\theta\frac{dH}{dx} + \frac{\partial\tilde{H}}{\partial\ \ell n\ R_\theta}\theta\frac{d\ \ell n\ R_\theta}{dx} \tag{118}$$

$$\theta\frac{d\tilde{H}}{dx} = \frac{\partial\tilde{H}}{\partial H}\theta\frac{dH}{dx} + \frac{\partial\tilde{H}}{\partial\ \ell n\ R_\theta}\left[\frac{\tau_w}{\rho U^2} - (H+1)\frac{\theta}{U}\frac{dU}{dx}\right] \tag{119}$$

and finally

$$\theta\frac{dH}{dx} = (H+1)\left(\tilde{H} + \frac{\partial\tilde{H}}{\partial\ \ell n\ R_\theta}\right)\frac{\partial H}{\partial\tilde{H}}\frac{\theta}{U}\frac{dU}{dx}$$

$$- \left(\tilde{H} + \frac{\partial\tilde{H}}{\partial\ \ell n\ R_\theta} - \hat{E}\right)\frac{\partial H}{\partial\tilde{H}}\frac{\tau_w}{\rho U^2} \tag{120}$$

where

$$\hat{E} \equiv \frac{\frac{E}{\tau_w}}{\rho\ U^2} = -\left[\frac{\partial(\tau/\tau_w)}{\partial(u/U)}\right]_\delta \tag{121}$$

Then from Equation (82)

$$M = -\ (H+1)\left(\tilde{H} + \frac{\partial\tilde{H}}{\partial\ \ell n\ R_\theta}\right)\frac{\partial H}{\partial\tilde{H}} \tag{122}$$

$$N = -\left(\tilde{H} + \frac{\partial\tilde{H}}{\partial\ \ell n\ R_\theta}\right)\frac{\partial H}{\partial\tilde{H}} \tag{123}$$

$$P = -\ \frac{\partial H}{\partial\tilde{H}} \tag{124}$$

and $\hat{E}_e$ is obtained from Equation (86) since $\hat{E}_e = \hat{C}_{S,e}$ for the entrainment method.

The actual evaluation of $\hat{E}_e$ and the accompanying shape parameter equation depends on the particular relation for entrainment thickness. Some examples are now presented:

POWER-LAW ENTRAINMENT THICKNESS

Here

$$\tilde{H} = \frac{2H}{H-1} \tag{63}$$

Then

$$\frac{d\tilde{H}}{dH} = -\ \frac{2}{(H-1)^2} \tag{125}$$

$$M = -\ H\left(H^2-1\right) \tag{126}$$

$$N = H(H-1) \tag{127}$$

$$P = \frac{(H-1)^2}{2} \tag{128}$$

and

$$\hat{E}_e = \frac{2H}{(H-1)}\left[\frac{(H+1)\beta}{H} + 1\right] + \frac{2A\ [H+(H+1)\beta]}{GH + A(H-1)^2} \tag{129}$$

HEAD ENTRAINMENT THICKNESS

Here

$$\tilde{H} = 1.535\ (H-0.7)^{-2.715} + 3.3 \tag{64}$$

Then

$$\frac{d\tilde{H}}{dH} = -\ 4.168\ (H-0.7)^{-3.715} \tag{130}$$

$$M = 0.3683\ (H+1)(H-0.7)\left[1 + 2.15\ (H-0.7)^{2.715}\right] \tag{131}$$

$$N = 0.3683\ (H-0.7)\left[1 + 2.164(H-0.7)^{2.715}\right] \tag{132}$$

$$P = \frac{(H-0.7)^{3.715}}{4.168} \tag{133}$$

and

$$E_e = \left[\frac{(H+1)\beta}{H} + 1\right]\tilde{H} - \left\{\frac{A(H-1)^2\quad H+(H+1)\beta}{GH + A(H-1)^2}\right\} \tag{134}$$

TWO-PARAMETER ENTRAINMENT THICKNESS

Here

$$\tilde{H} = \frac{H(H+2)}{2(H-1)} + \frac{3.8\ H^{7/2}}{(H-1)^{5/2}}\left(\frac{\tau_w}{\rho\ U^2}\right)^{3/4} \tag{69}$$

With Equation (25)

$$\frac{\partial\tilde{H}}{\partial H} = \frac{H^2-2H-2}{2(H-1)^2} + \frac{3.8\ H^{7/2}}{(H-1)^{5/2}}\left(\frac{\tau_w}{\rho\ U^2}\right)^{3/4}\left[\frac{2H-7}{2H(H-1)} - \frac{3c_2}{2.3\left(H_o+1\right)H\gamma}\right] \tag{135}$$

and with Equations (37) and (42)

$$\frac{\partial\tilde{H}}{\partial\ \ell n\ R_\theta} = -\ \frac{5.7\ H^{7/2}}{(H-1)^{5/2}}\left(\frac{\tau_w}{\rho\ U^2}\right)^{3/4}\left[\frac{\alpha_1}{2.3}\left(\frac{\tau_w}{\rho\ U^2}\right)_o^{1/2} + \frac{2\alpha\left(H_o-1\right)^2}{2.3\left(H_o+1\right)}\left(\frac{c_2}{2.3H_o\gamma_o} - \frac{\ell n\ \frac{\gamma}{\gamma_o}}{H_o+1}\right)\right] \tag{136}$$

M, N, P, and E_e are obtained from Equations (122), (123), (124), and (86). Figure 5 shows large differences in M between the various formulations.

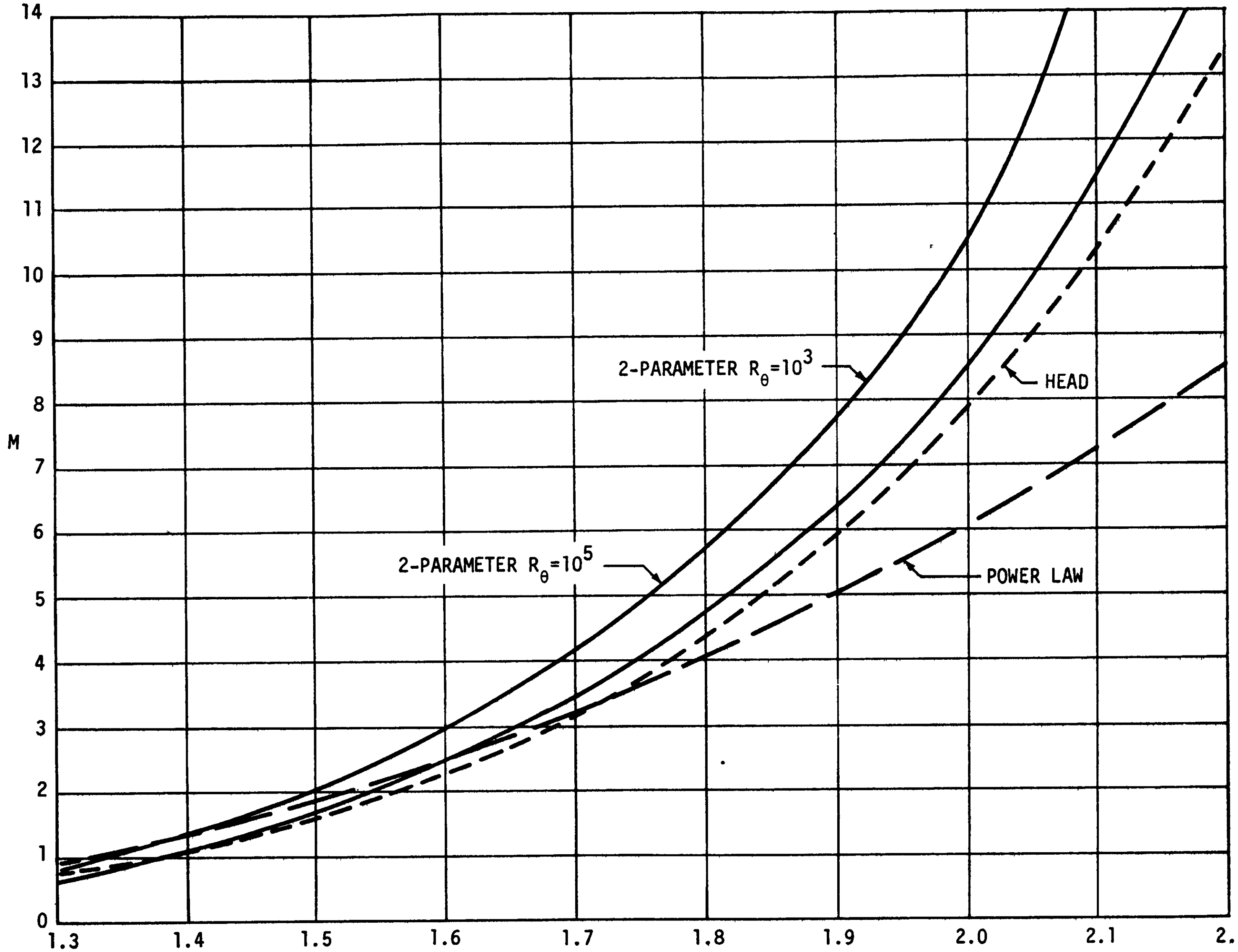

Figure 5 - Entrainment Method, $M = f[H, R_\theta]$; Comparison of Various Procedures

EXISTING RELATIONS FOR ENTRAINMENT FACTOR

Empirically Head[4] obtains

$$E = 0.0306 \left[1.535(H-0.7)^{-2.715} + 0.3\right]^{-0.653} \tag{137}$$

Also Nicoll and Ramaprian[30] include Statford's data for separating flow and obtain an empirical fit

$$E = 0.035 \sqrt{H-1.25} \tag{138}$$

Figure 6 compares the various entrainment factors.

PARTIAL MOMENTUM METHODS

GENERAL

Another group of integrated equations which are transformable into shape parameter equations may be obtained by integrating the equation of motion, Equation (78), to some intermediate value of y, say s[x]. s may be $s = m\delta$ where m is a constant which was used by Moses[4] or $s = \theta$ which was used by Furuya and Nakamura.[4] Another possibility is s[u/U = const] which will not be treated here.

Integrating the equation of motion, Equation (78), to y = s produces

$$\frac{d}{dx} \int_0^s \left(\frac{u}{U}\right)^2 dy - \frac{u_s}{U} \int_0^s \frac{u}{U}\, dy + \left[2 \int_0^s \left(\frac{u}{U}\right)^2 dy - \frac{u_s}{U} \int_0^s \frac{u}{U}\, dy - s\right] \frac{1}{U}\frac{dU}{dx} =$$

$$= \frac{\tau_s}{\rho U^2} - \frac{\tau_w}{\rho U^2} \tag{139}$$

where

$$u_s = u \text{ at } y = s$$

$$\tau_s = \tau \text{ at } y = s.$$

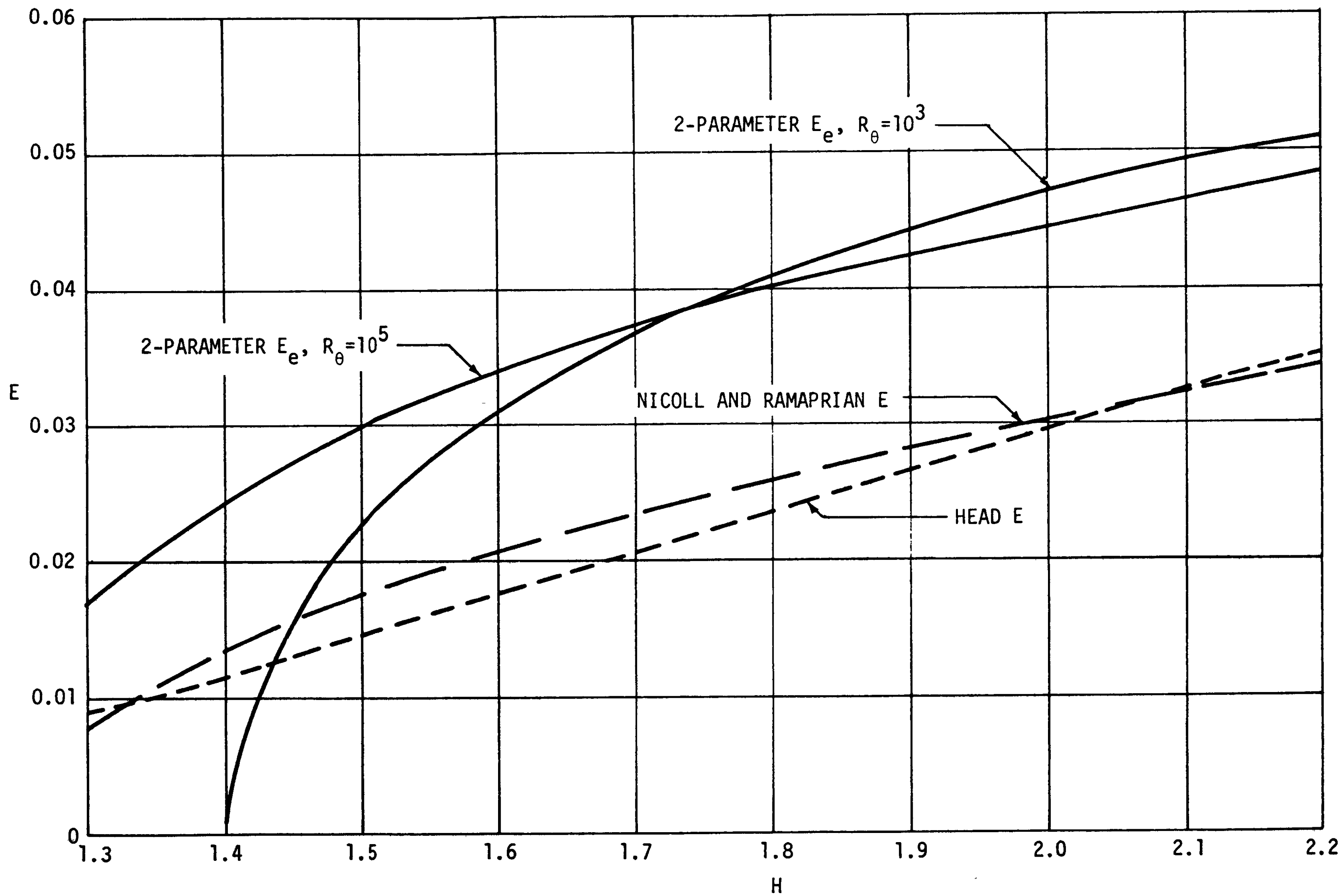

Figure 6 - Entrainment Method, $E = f[H, R_\theta]$; Comparison of Various Procedures

Two new shape parameters are introduced:

$$\hat{H} \equiv \frac{\int_o^s \frac{u}{U}\, dy}{\theta} \tag{140}$$

and

$$\bar{H} \equiv \frac{\int_o^s \left(\frac{u}{U}\right)^2 dy}{\theta} \tag{141}$$

Then Equation (139) becomes

$$\frac{d}{dx}(\bar{H}\theta) - \frac{u_s}{U}\frac{d}{dx}(\hat{H}\theta) + \left(2\bar{H} - \frac{u_s}{U}\hat{H} - \frac{s}{\theta}\right)\frac{\theta}{U}\frac{dU}{dx}$$

$$= \frac{\tau_s}{\rho\, U^2} - \frac{\tau_w}{\rho\, U^2} \tag{142}$$

With

$$\hat{H} = f\left[H, \ell n\ R_\theta\right] \tag{143}$$

and

$$\bar{H} = f\left[H, \ell n\ R_\theta\right] \tag{144}$$

$$\theta\frac{dH}{dx} = \left\{\frac{H\bar{H} + (H+1)\left[\frac{\partial\bar{H}}{\partial\ \ell n\ R_\theta} - \frac{u_s}{U}\left(\hat{H} + \frac{\partial\hat{H}}{\partial\ \ell n\ R_\theta}\right)\right] + \frac{s}{\theta}}{\frac{\partial\bar{H}}{\partial H} - \frac{u_s}{U}\frac{\partial\hat{H}}{\partial h}}\right\}\frac{\theta}{U}\frac{dU}{dx}$$

$$- \left[\frac{\bar{H} + \frac{\partial\bar{H}}{\partial\ \ell n\ R_\theta} - \frac{u_s}{U}\left(\hat{H} + \frac{\partial\hat{H}}{\partial\ \ell n\ R_\theta}\right) + 1 - \frac{\tau_s}{\tau_w}}{\frac{\partial\bar{H}}{\partial H} - \frac{u_s}{U}\frac{\partial\hat{H}}{\partial H}}\right]\frac{\tau_w}{\rho\, U^2} \tag{145}$$

Then

$$M = -\frac{H\bar{H} + (H+1)\left[\frac{\partial \bar{H}}{\partial \ \ell n \ R_\theta} - \frac{u_s}{U}\left(\hat{H} + \frac{\partial \hat{H}}{\partial \ \ell n \ R_\theta}\right)\right] + \frac{s}{\theta}}{\frac{\partial \bar{H}}{\partial H} - \frac{u_s}{U}\frac{\partial \hat{H}}{\partial H}} \tag{146}$$

$$N = -\frac{\bar{H} + \frac{\partial \bar{H}}{\partial \ \ell n \ R_\theta} - \frac{u_s}{U}\left(\hat{H} + \frac{\partial \hat{H}}{\partial \ \ell n \ R_\theta}\right) + 1}{\frac{\partial \bar{H}}{\partial H} - \frac{u_s}{U}\frac{\partial \hat{H}}{\partial H}} \tag{147}$$

$$P = -\left(\frac{\partial \bar{H}}{\partial H} - \frac{u_s}{U}\frac{\partial \hat{H}}{\partial H}\right)^{-1} \tag{148}$$

$$\hat{C}_S = \frac{\tau_s}{\tau_w} \tag{149}$$

POWER-LAW VELOCITY PROFILE ($s = m\delta$)

For power-law velocity profiles Equation (16)

$$\hat{H} = \frac{2H}{H-1}\left(\frac{s}{\delta}\right)^{\frac{H+1}{2}} \tag{150}$$

and for $s = m\delta$

$$\hat{H} = \frac{2H}{H-1} m^{\frac{H+1}{2}} \tag{151}$$

and

$$\frac{d\hat{H}}{dH} = -\frac{m^{\frac{H+1}{2}}}{(H-1)^2}\left[2 - H(H-1) \ \ell n \ m\right] \tag{152}$$

Since

$$\frac{u_s}{U} = \left(\frac{s}{\delta}\right)^{\frac{H-1}{2}} \tag{153}$$

$$\frac{u_s}{U} = m^{\frac{H-1}{2}} \tag{154}$$

For power-law velocity profiles

$$\bar{H} = \left(\frac{H+1}{H-1}\right)\left(\frac{s}{\delta}\right)^{H} \tag{155}$$

and for $s = m_{\delta}$

$$\bar{H} = \left(\frac{H+1}{H-1}\right) m^{H} \tag{156}$$

$$\frac{d\bar{H}}{dH} = -\frac{m^{H}}{(H-1)^{2}}\left[2 - \left(H^{2}-1\right)\ \ell n\ m\right] \tag{157}$$

Therefore from Equations (146), (147), and (148)

$$M = \frac{H(H+1)}{\ell n\ m}\left(1 - m^{1-H}\right) \tag{158}$$

$$N = \frac{(H-1)}{\ell n\ m}\left(1+m^{-H}\right) \tag{159}$$

$$P = -\frac{(H-1)}{m^{H}\ \ell n\ m} \tag{160}$$

POWER-LAW VELOCITY PROFILE ($s = \theta$)

From Equations (150) and (19)

$$\hat{H} = \frac{2H}{(H-1)}\left[\frac{H-1}{H(H+1)}\right]^{\frac{H+1}{2}} \tag{161}$$

and

$$\frac{d\hat{H}}{dH} = \left[\frac{H-1}{H(H+1)}\right]^{\frac{H+1}{2}}\left\{\frac{H}{H-1}\ \ell n\left[\frac{H-1}{H(H+1)}\right] - 1\right\} \tag{162}$$

Also

$$\frac{u_s}{U} = \left[\frac{H-1}{H(H+1)}\right]^{\frac{H-1}{2}} \tag{163}$$

$$\bar{H} = \frac{1}{H}\left[\frac{H-1}{H(H+1)}\right]^{H-1} \tag{164}$$

and

$$\frac{d\bar{H}}{dH} = -\frac{1}{H}\left[\frac{H-1}{H(H+1)}\right]^{H-1}\left\{\frac{H-1}{H+1} - \ln\left[\frac{H-1}{H(H+1)}\right]\right\} \tag{165}$$

Then

$$M = \frac{H(H+1) - (H-1)\left[\frac{H-1}{H(H+1)}\right]^{-H}}{\ln\left[\frac{H-1}{H(H+1)}\right]} \tag{166}$$

$$N = \frac{(H-1)\left\{1 - \left[\frac{H-1}{H(H+1)}\right]^{-H}\right\}}{\ln\left[\frac{H-1}{H(H+1)}\right]} \tag{167}$$

$$P = -\frac{H-1}{\left[\frac{H-1}{H(H+1)}\right]^{H} \ln\left[\frac{H-1}{H(H+1)}\right]} \tag{168}$$

TWO-PARAMETER VELOCITY PROFILE ($s = m\delta$)

The objective is to obtain $\tilde{H}\left[H,R_\theta\right]$ and $\bar{H}\left[H,R_\theta\right]$. Let us introduce shape parameter $\hat{G}$ defined as

$$\hat{G} \equiv \frac{\int_o^{s/\delta}\left(\frac{U-u}{u_\tau}\right) d\left(\frac{y}{\delta}\right)}{\int_o^1\left(\frac{U-u}{u_\tau}\right) d\left(\frac{y}{\delta}\right)} \tag{169}$$

From appropriate definitions

$$\hat{H} = \left(\frac{\delta}{\theta}\right)\left(\frac{s}{\delta}\right) - H\hat{G} = \left(\tilde{H}+H\right)\left(\frac{s}{\delta}\right) - H\hat{G} \tag{170}$$

Then for $s = m\delta$

$$\hat{H} = (\tilde{H}+H)m - H\hat{G} \tag{171}$$

Likewise let us introduce shape parameter $\bar{G}$ defined as

$$\bar{G} \equiv \frac{\int_{o}^{s/\delta} \left(\frac{U-u}{u_{\tau}}\right)^{2} d\left(\frac{y}{\delta}\right)}{\int_{o}^{1} \left(\frac{U-u}{u_{\tau}}\right) d\left(\frac{y}{\delta}\right)} \tag{172}$$

From appropriate definitions

$$\bar{H} = (H-1)\,\frac{\bar{G}}{G} + \left(\frac{\delta}{\theta}\right)\left(\frac{s}{\delta}\right) -2\,H\hat{G} = (H-1)\,\frac{\bar{G}}{G} + (\tilde{H}+H)\,\frac{s}{\delta} -2\,H\hat{G} \tag{173}$$

For $s = m\delta$

$$\bar{H} = (H-1)\,\frac{\bar{G}}{G} + (\tilde{H}+H)m -2\,H\hat{G} \tag{174}$$

From the law of the wake, Equation (12)

$$\hat{G} = \frac{A\ m(1-\ell n\ m) + B_2\ m\left[1 - m^2\left(1 - \frac{m}{2}\right)\right]}{A + \frac{1}{2}B_2} \tag{175}$$

$\hat{G}$ is related to G through B_2 in Equation (23).

An empirical fit for m = 0.3 (m = 0.3 was used by Moses) gives

$$\hat{G}_{0.3} = 0.5541 + \frac{0.410}{G} \tag{176}$$

or from Equation (22)

$$\hat{G}_{0.3} = 0.5541 + 0.410\,\frac{H}{(H-1)}\left(\frac{\tau_w}{\rho\ U^2}\right)^{\frac{1}{2}} \tag{177}$$

Unfortunately the condition $s = \theta$ does not lend itself to this type of analysis.

Then

$$\hat{H}_{0.3} = 0.3(\tilde{H}+H) -H\left[0.5541 + \frac{0.410H}{H-1}\sqrt{\frac{\tau_w}{\rho\ U^2}}\ \right] \tag{178}$$

Since

$$I_1 \bar{G} = \int_o^m \left(\frac{U-u}{u_\tau}\right)^2 d\left(\frac{y}{\delta}\right)$$

consequently

$$\begin{aligned} I_1 \bar{G} = {} & A^2 m\left(\ell n^2 m - 2 \ell n m + 2\right) - 2 A B_2 m(\ell n m - 1) \\ & + A B_2 m^3 \left[(2-m) \ell n m + \frac{1}{4} m - \frac{2}{3}\right] \\ & + B_2{}^2 m \left(1 - 2m^2 + m^3 + \frac{9}{5} m^4 - 2 m^5 + \frac{4}{7} m^6\right) \end{aligned} \tag{179}$$

For m = 0.3

$$I_1 \bar{G}_{0.3} = 1.7573 A^2 + 1.2512 A B_2 + 0.2571 B_2{}^2 \tag{180}$$

$\bar{G}$ is related to G through B_2 by Equation (23). An empirical fit gives for m = 0.3

$$\frac{\bar{G}_{0.3}}{G} = 0.686 + \frac{2.04}{G^2} \tag{181}$$

or

$$\frac{\bar{G}_{0.3}}{G} = 0.686 + \frac{2.04 H^2}{(H-1)^2} \frac{\tau_w}{\rho U^2} \tag{182}$$

Then from Equation (174)

$$\bar{H}_{0.3} = 0.3 \tilde{H} - 0.122 H - 0.686 - \frac{0.820 H^2}{H-1} \sqrt{\frac{\tau_w}{\rho U^2}} \left(1 - 2.488 \sqrt{\frac{\tau_w}{\rho U^2}}\right) \tag{183}$$

From Equation (10) for $m = s/\delta$

$$\frac{u_s}{U} = 1 - \sqrt{\frac{\tau_w}{\rho U^2}} \left[- A \ell n m + B_2 \left(1 - \frac{1}{2} w[m]\right)\right] \tag{184}$$

A linearized fit of Equation (23) yields

$$B_2 = 1.364\ (G - 4.78) \tag{185}$$

Then for m = 0.3

$$\left(\frac{u}{U}\right)_{0.3} = 1 - 1.069\ \frac{(H-1)}{H} + 2.232\sqrt{\frac{\tau_w}{\rho\ U^2}} \tag{186}$$

Now from Equation (183)

$$\frac{\partial \bar{H}_{0.3}}{\partial H} = 0.3\ \frac{\partial \tilde{H}}{\partial H} - 0.122 - \frac{0.820H}{(H-1)}\sqrt{\frac{\tau_w}{\rho\ U^2}}\left[\frac{(H-2)}{(H-1)}\left(1 - 2.488\sqrt{\frac{\tau_w}{\rho\ U^2}}\right) - \frac{2\ c_2}{2.3(H_o+1)\gamma}\left(1 - 4.976\sqrt{\frac{\tau_w}{\rho\ U^2}}\right)\right] \tag{187}$$

and from Equation (178)

$$\frac{\partial \hat{H}_{0.3}}{\partial H} = 0.3\ \frac{\partial \tilde{H}}{\partial H} - 0.2541 - \frac{0.410H}{H-1}\sqrt{\frac{\tau_w}{\rho\ U^2}}\left[\frac{H-2}{H-1} - \frac{2\ c_2}{2.3(H_o+1)\gamma}\right] \tag{188}$$

Also

$$\frac{\partial \bar{H}_{0.3}}{\partial\ \ell n\ R_\theta} = \frac{0.820H^2}{(H-1)}\sqrt{\frac{\tau_w}{\rho\ U^2}}\left[1 - 6.07\sqrt{\frac{\tau_w}{\rho\ U^2}} - 2.08\left(\frac{H}{H-1}\right)^{3/2}\left(\frac{\tau_w}{\rho\ U^2}\right)^{\frac{1}{4}}\right] \text{x}$$
$$\text{x}\left[\frac{\alpha_1}{2.3}\left(\frac{\tau_w}{\rho\ U^2}\right)_0^{1/2} + \frac{2a\left(H_o-1\right)^2}{2.3\left(H_o+1\right)}\left(\frac{c_2}{2.3H_o\gamma_o} - \frac{\ell n\ \frac{\gamma}{\gamma_o}}{H_o+1}\right)\right] \tag{189}$$

and

$$\frac{\partial \hat{H}_{0.3}}{\partial\ \ell n\ R_\theta} = \frac{0.410H^2}{(H-1)}\sqrt{\frac{\tau_w}{\rho\ U^2}}\left[1 - 4.17\left(\frac{H}{H-1}\right)^{3/2}\left(\frac{\tau_w}{\rho\ U^2}\right)^{1/4}\right] \text{x}$$
$$\text{x}\left[\frac{\alpha_1}{2.3}\left(\frac{\tau_w}{\rho\ U^2}\right)_o^{1/2} + \frac{2a\left(H_o-1\right)^2}{2.3\left(H_o+1\right)}\left(\frac{c_2}{2.3H_o\gamma_o} - \frac{\ell n\ \frac{\gamma}{\gamma_o}}{H_o+1}\right)\right] \tag{190}$$

If the equation of motion, Equation (78), is multiplied by y and then integrated from y = 0 to y = δ, a moment of momentum equation is formed. Unfortunately the resulting equation is awkward to deal with on the basis of the two-parameter velocity profile in order to obtain a shape parameter equation. However a convenient form results from a power-law velocity profile which Tetervin and Lin[31] originally obtained

$$\theta \frac{dH}{dx} = -\frac{H(H+1)(H^2-1)}{2} \frac{\theta}{U} \frac{dU}{dx} + H \left(H^2-1\right) \frac{\tau_w}{\rho U^2} - \frac{(H+1)(H^2-1)}{2} C_\tau \tag{191}$$

where

$$C_\tau \equiv 2 \int_0^1 \frac{\tau}{\rho U^2} d\left(\frac{y}{\delta}\right) \tag{192}$$

is the shear-stress integral.

From Equation (83)

$$M = \frac{H(H+1)(H^2-1)}{2} \tag{193}$$

$$N = H H^2-1 \tag{194}$$

$$P = \frac{(H+1)(H^2-1)}{2} \tag{195}$$

Then from Equation (86)

$$C_{\tau,e} = \left\{\beta + \frac{2H}{H+1} + \frac{2A[H+(H+1) \beta](H-1)}{(H+1)^2[GH+A H-1]^2}\right\} \frac{\tau_w}{\rho U^2} \tag{196}$$

Nash and Hicks[4] use

$$C_{\tau,e} = 0.025 \left(1 - \frac{1}{H}\right)^2 \tag{197}$$

while Nash and Macdonald[32] suggest

$$C_{\tau,e} = (\beta + 1.16) \frac{\tau_w}{\rho U^2} \tag{198}$$

Also McDonald[33] proposes

$$C_{\tau,e} = (0.93\ \beta + 1.2) \frac{\tau_w}{\rho U^2} \tag{199}$$

Values of C_τ for strong adverse pressure gradients are given in Reference 12 as

$$C_\tau = \left(\frac{H-1}{H+1}\right)2\ \psi_o \tag{200}$$

where

$$\psi_o = \frac{H_o}{\left(H_o - 1\right)} \left[1 + \frac{0.0378\ \sqrt{52.9 \log H_o - 4.18}}{H_o^{\ 2} - 1}\right] \left(\frac{\tau_w}{\rho U^2}\right)_o \tag{201}$$

Figure 7 compares the shear stress integrals of some of the various formulations.

NONEQUILIBRIUM PRESSURE GRADIENTS

The use of equilibrium stress factors not only ensures agreement for equilibrium pressure gradients but also for quasi-equilibrium conditions where the G values do not remain constant but vary in accordance with the equilibrium G-β relation. Relating equilibrium stress factors to H and R_θ provides a built-in lag which is characteristic of the response of the shear-stress distribution to sudden changes in pressure gradients. Lag-type equations have been proposed by Goldberg[21] and Nash and Hicks[4] of type

$$\delta \frac{d\ C_S}{dx} = \lambda \left(C_{S,e} - C_S\right) \tag{202}$$

where λ is a constant adjusted to suit the experimental data.

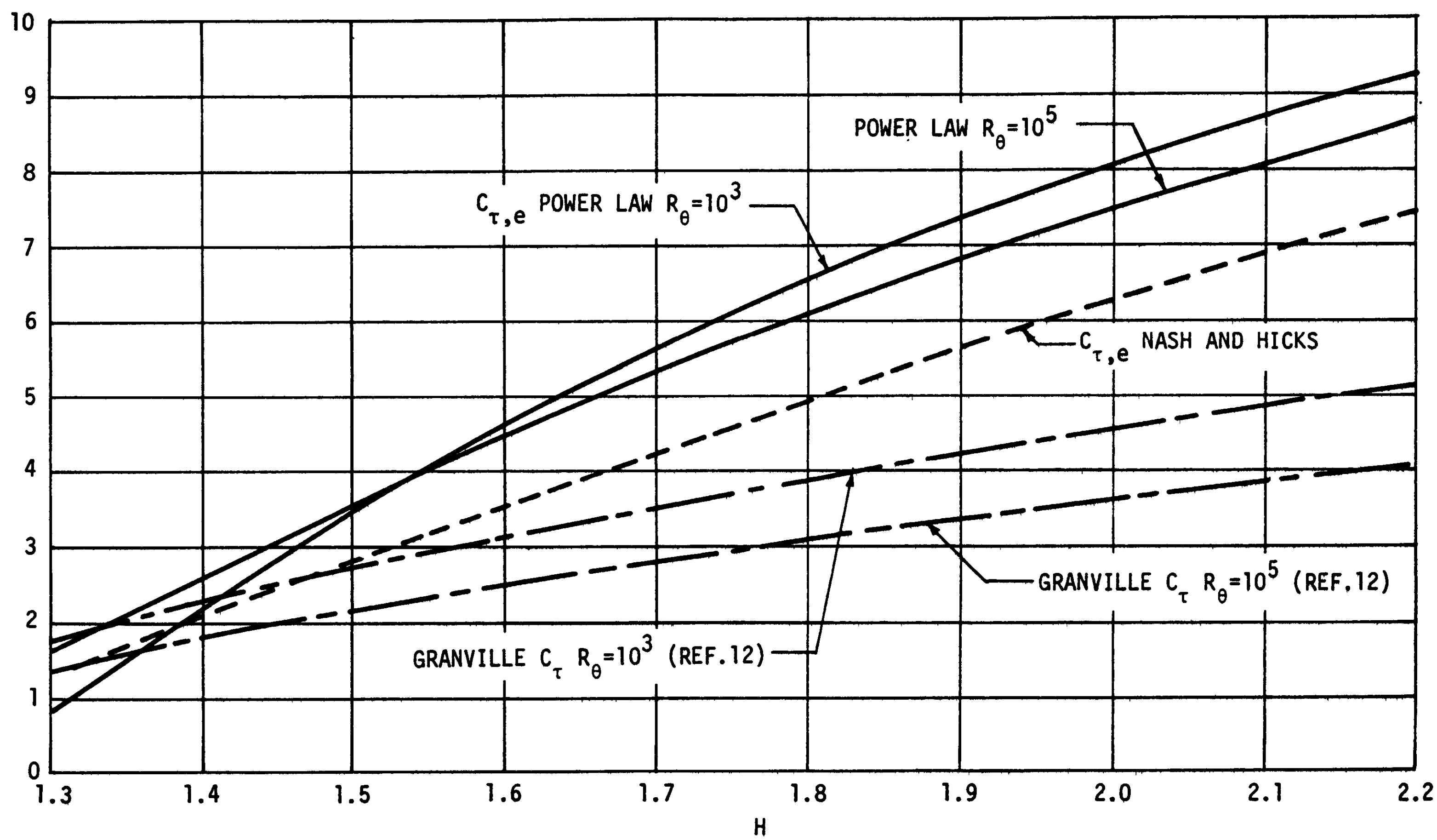

Figure 7 - Moment of Momentum Method, $C_\tau = f[H, R_\theta]$; Comparison of Various Procedures

Close to separation ordinary boundary layer conditions seem to fail. There are three-dimensional cross flows, normal-stress effects and normal pressure variations. This region merits a study of its own.

REFERENCES

1. Rotta, J.C., "Turbulent Boundary Layers in Incompressible Flow," in "Progress in Aeronautical Sciences," Vol. 2, A. Ferri et al., eds., Pergamon Press, New York (1962).

2. Rotta, J.C., "Critical Review of Existing Methods for Calculating the Development of Turbulent Layers" in "Fluid Mechanics of Internal Flow," G. Sovran, ed., Elsevier Publishing Co., Amsterdam (1967) (Proceedings of General Motors Symposium (1965).

3. Rotta, J.C., "Recent Developments in Calculation Methods for Turbulent Boundary Layers with Pressure Gradients and Heat Transfer," Transactions of ASME, J. Appl. Mech., Series E, Vol. 33, No. 2 (Jun 1966).

4. Kline, S.J. et al., eds., "Proceedings - Computation of Turbulent Boundary Layers - 1968 AFOSR-IFP-Stanford Conference," Vol. 1, Thermosciences Div., Dept. Mech. Eng., Stanford University, Calif. (1968).

5. Mickley, H.S. et al., "Nonequilibrium Turbulent Boundary Layer," AIAA Journal, Vol. 5, No. 9 (Sep 1967).

6. McDonald, H. and Stoddart, J.A.P., "On the Development of the Incompressible Turbulent Boundary Layer," British Aircraft Corp. Ae 225 (Mar 1965); also ARC R&M 3484 (1967).

7. Patel, V.C., "Calibration of the Preston Tube and Limitations on its Use in Pressure Gradients," J. Fluid Mech., Vol. 23, Pt. 1 (Sep 1965).

8. Coles, D., "The Law of the Wake in the Turbulent Boundary Layer," J. Fluid Mech., Vol. 1, Pt. 2 (Jul 1956).

9. Hinze, J.O., "Turbulence," McGraw-Hill, New York (1959).

10. Moses, H.L., "The Behavior of Turbulent Boundary Layers in Adverse Pressure Gradients," Gas Turbine Laboratory, Massachusetts Institute of Technology Report 73 (Jan 1964).

11. Rotta, J., "On the Theory of the Turbulent Boundary Layer," Mitteilungen aus dem Max-Plank-Institut für Strömungsforschung, No. 1 (1950); translated as NACA TM 1344 (Feb 1953).

12. Granville, P.S., "A Method for the Calculation of the Turbulent Boundary Layer in a Pressure Gradient," David Taylor Model Basin Report 752 (May 1951).

13. Patel, R.P., "An Improved Law for the Skin Friction in an Incompressible Turbulent Boundary Layer in any Pressure Gradient," Dept. of Mech. Eng., McGill University (May 1962).

14. Ludwieg, H. and Tillmann, W., "Investigations of Surface Shearing Stresses in Turbulent Boundary Layers," Ingenieur-Archiv, Vol. 17, No. 4, p. 288 (1949); translated as NACA TM 1285 (May 1950).

15. Uram, E.M., "Skin-Friction Calculation for Turbulent Boundary Layers in Adverse Pressure Distributions," J. Aero. Sci., Vol. 27, p. 75 (1960).

16. Felsch, K.O., "A Contribution to the Calculation of Turbulent Boundary Layers in Two-Dimensional Incompressible Flow," Deutsche Luft-und Raumfahrt Forschungsbericht 66-46 (July 1966), Royal Aircraft Establishment Library Translation 1219 (Mar 1967).

17. Nash, J.F., "A Note on Skin-Friction Laws for the Incompressible Turbulent Boundary Layer," National Physical Laboratory Aerodynamics Division Report 1135 (Dec 1964).

18. Wieghardt, K. and Tillmann, W., "On the Turbulent Friction Layer for Rising Pressure," Kaiser Wilhelm - Institut für Strömungsforschung ZWB U&M 6617 (Nov 1964); translated as NACA TM 1314 (Oct 1951).

19. Fernholz, H., "A New Empirical Relationship between the Form-Parameters H_{32} and H_{12} in Boundary Layer Theory," J. Royal Aer. Soc., Vol. 66, No. 9 (Sep 1962).

20. Moses, H.L. et al., "Boundary Layer Separation in Internal Flow," Gas Turbine Laboratory, Massachusetts Institute of Technology Report 81 (Sep 1965).

21. Goldberg, P., "Upstream History and Apparent Stress in Turbulent Boundary Layers," Gas Turbine Laboratory, Massachusetts Institute of Technology Report 85 (May 1966).

22. Nicoll, W.B. and Escudier, M.P., "Empirical Relationships between the Shape Factors H_{32} and H_{12} for Uniform-Density Turbulent Boundary Layers and Wall Jets," AIAA Journal, Vol. 4, No. 5 (May 1966).

23. Nash, J.F., "Turbulent-Boundary-Layer Behavior and the Auxiliary Equation," in "Recent Developments in Boundary Layer Research," AGARDograph 97 (May 1965).

24. Alber, I.E., "Turbulent Boundary Layer Development," Dynamic Science Co. TR-A68-101, Monrovia, Calif. (Jan 1968).

25. Truckenbrodt, E., "A Method of Quadrature for Calculation of the Laminar and Turbulent Boundary Layer in Case of Plane and Rotationally Symmetrical Flow," Ingenieur-Archiv, Vol. 20 (1952); translated as NACA TM 1379 (May 1955).

26. Walz, A., "Über Fortschritte in Näherungstheorie und Praxis der Berechnung Kompressibler laminarer und turbulenter Grenzschichten mit Warmeübergang," Zeitschrift für Flugwissenschaften, Vol. 13, No. 3 (Mar 1965).

27. Escudier, M.P. and Spalding, D.B., "A Note on the Turbulent Uniform-Property Hydrodynamic Boundary Layer on a Smooth Impermeable Wall; Comparisons of Theory with Experiment," (AD-805492) ARC Current Paper 815 (1966).

28. Escudier, M.P. et al., "Decay of a Velocity Maximum in a Turbulent Boundary Layer," Aero. Quarterly, Vol. 18, Pt. 2 (May 1967).

29. Head, M.R., "Entrainment in the Turbulent Boundary Layer," ARC R&M 3152 (Sep 1958).

30. Nicoll, W.B. and Ramaprian, B.R., "A Modified Entrainment Theory for the Prediction of Turbulent Boundary Layer Growth in Adverse Pressure Gradients," ASME Transactions, J. Bas. Eng. Vol. 91, Series D, No. 4 (Dec 1969).

31. Tetervin, N. and Lin, C.C., "A General Integral Form of the Boundary-Layer Equation for Incompressible Flow with an Application to the Calculation of the Separation Point of Turbulent Boundary Layers," NACA Report 1046 (1951).

32. Nash, J.F. and Macdonald, A.G.J., "A Calculation Method for the Incompressible Turbulent Boundary Layer, Including the Effect of Up-stream History of the Turbulent Shear Stress," National Physical Laboratory Aero Report 1234 (May 1967).

33. McDonald, H., "The Departure from Equilibrium of Turbulent Boundary Layers," Aero. Quarterly, Vol. 19, Pt. 1 (Feb 1968).

INITIAL DISTRIBUTION

Copies	
3	NAVORDSYSCOM 1 Weapons Dyn Div (NORD 035) 2 Torpedo Div (NORD 054131)
5	NAVSHIPSYSCOM 2 SHIPS 2052 1 SHIPS 031 1 SHIPS 03412 1 SHIPS 3211
2	DSSPO 1 Ch Sci (PM 11-001) 1 Vehicles Br (PM 11-22)
4	NAVSEC 1 SEC 6110.01 1 SEC 6114 1 SEC 6114D 1 SEC 6115
2	NAVAIRSYSCOM
4	CHONR 3 Fluid Dyn Br (ONR 438) 1 Nav Appl Div (ONR 460)
1	CO & D, USNUSL
1	CO & D, USNELC
6	CO & D, USNOL 1 Dr. R.E. Wilson 1 Dr. A.E. Seigel 1 Dr. V.C. Dawson 1 Dr. A. May 1 N. Tetervin
5	CDR, USNUWC (Pasadena) 1 Dr. J.W. Hoyt 1 Dr. A.G. Fabula 1 Dr. T. Lang 1 Dr. J.G. Waugh
2	CDR, NWC (China Lake) 1 Dr. H. Kelly
1	Dir, USNRL
5	CO, USNAVUWRES (Newport) 1 R.J. Grady 1 P. Gibson 1 J.F. Brady 1 R.H. Nadolink
2	AFOSR 1 Mech Div (Maj. Calvert) (518)

Copies	
1	BuStds Attn: Hydraulic Lab
20	CDR, DDC
1	MARAD (Div of Ships Des & Dev)
1	CO, US Army Transp R&D Comm (Fort Eustis, Va) (Marine Transp Div)
2	NASA Hdqtrs. 1 A. Gessow
1	Dir Eng Sci Div Nat Sci Found, Washington, D.C.
1	SNAME 74 Trinity Place, New York, N.Y. 10006
1	Webb Inst of Nav Arch Crescent Beach Rd, Glen Cove, L.I., N.Y.
5	ORL, Penn St. 1 Dr. G.F. Wislicenus 1 Dr. J.L. Lumley 1 Dr. M. Sevik 1 R.E. Henderson
1	Univ of Mich, Ann Arbor Dept of Nav Arch
2	Univ of Calif, Berkeley Dept of Nav Arch
2	Alden Res Lab Worchester, Mass 1 Dr. L.J. Hooper 1 L.C. Neale
1	Prof L. Landweber Iowa Inst of Hydraulic Res State Univ of Iowa, Iowa City, Iowa
1	Prof E.Y. Hsu, Dept Civil Eng Stanford Univ, Stanford, Calif
1	Prof S.J. Kline, Dept of Mech Eng, Stanford Univ, Stanford, Calif

Copies

4 MIT, Dept Naval Arch
Attn: Dr. J.N. Newman,
P. Mandel, Prof M. Abkowitz

1 Prof Frank M. White
Dept of Mech Eng, Univ of R.I.
Kingston, R.I.

1 Prof A.J. Acosta
Hydrodynamics Lab, CIT,
Pasadena, Calif

4 Dept Mech Eng
Catholic Univ, Wash., D.C.
1 Prof M.J. Casarella
1 Prof P.K. Chang
1 Prof Kelnhofer

1 Dr. C.S. Wells, Jr.
LTV Res Center, Dallas, Texas

2 St. Anthony Falls Hydr Lab
Univ of Minn., Minneapolis

3 Hydronautics, Inc., Laurel, Md.
1 Dr. B.L. Silverstein
1 M.P. Tulin

1 J. Levy, Hydrodynamics Dept
Aerojet-Gen, Azusa, Calif

1 Westinghouse Electr Corp,
Annapolis
Attn: M.S. Macovsky

1 Dr. E.R. van Driest
Ocean Systems Op
North American Rockwell Corp
Anaheim, Calif

1 Oceanics, Inc.
Attn: A. Lehman

1 Dr. R. Bernicker
Esso Math & Systems, Inc.
Florham Park, N.J.

1 Prof Douglas E. Abbott
Fluid Mechanics Lab
School of Mechanical Engrg
Purdue Univ
Lafayette, Indiana 47907

1 Mr. Irwin E. Alber
Dynamic Science
1900 Walker Ave
Monrovia, Calif 91019

Copies

2 Aerotherm
460 Calif Ave
Palo Alto, Calif
1 Mr. Robert N. Kendall
1 Mr. L. Anderson

1 Mr. Ivan Beckwith
NSAS Langley Research Center
Mail Drop-161
Langley Station
Hampton, Va 23365

1 Mr. T. Cebeci
Douglas Aircraft Div
3855 Lakewood Blvd
Long Beach, Calif 90801

1 Prof Francis H. Clauser
Vice Chancelor
Univ of Calif
Santa Cruz, Calif 95060

1 Prof Donald Coles, GALCIT
306 Karman Lab
CIT, Pasadena, Calif 91109

1 Prof G. Corcos
Dept of Mechanical Engrg
Div of Aeronautical Sci
Univ of Calif
Berkeley, Calif 94720

1 Dr. G. Deboy
Dept Mechanical Engr
Purdue Univ
Lafayette, Indiana 47907

1 Dr. George S. Deiwert
Ames Lab
Fluid Mechanics Br
Bldg 229-1, Mail Stop N-229-4
Moffett Field, Calif
94035

1 Dr. C. Donaldson
Aeronautical Research Assoc.
of Princeton, Inc
Princeton, N.J. 08540

1 Dr. F. Dvorak
Aero Research Staff
Mail Stop 55-38
Commercial Airplane Div
Boeing Company
Seattle, Wash.

Copies	
1	Prof Howard W. Emmons Rm 308, Pierce Hall Harvard Univ Cambridge, Mass. 02138
1	Prof M.P. Escudier, Rm 3-258 Dept Mechanical Engr, MIT Cambridge, Mass. 02139
1	Dr. V.G. Forsnes Dept Mech Engrg Purdue Univ Lafayette, Indiana 47907
1	Dr. Perry Goldberg Pratt & Whitney Aircraft Co East Hartford, Conn 06100
1	Dr. H. James Herring School of Engrg & Appl Sci Princeton Univ Princeton, N.J. 08540
1	Dr. Eric A. Hirst Dept of Mech Engrg Tuskegee Institute Alabama 36088
1	Prof James P. Johnston Mech Engrg Dept Thermosciences Div Stanford Univ Stanford, Calif 94305
1	Mr. J.S. Keith Senior Engr Mail Drop H-45 General Electric Co Cincinnati, Ohio 45215
1	Prof L.S.G. Kovasznay Dept Mechanics JHU (Homewood Campus) Baltimore, Md. 21218
1	Prof. Richard E. Kronauer Div of Engrg & Applied Physics, Pierce Hall 324 Harvard Univ Cambridge, Mass 02138
1	Prof H.W. Liepmann Karman Lab CIT, Pasadena, Calif 91109

Copies	
1	Prof John L. Lumley Aerospace Engrg Dept 153E Hammond Bldg Penn State Univ Univ Park, Pa 16802
1	Mr. H. McDonald Fluid Dynamics Lab United Aircraft Research Ctr Silver Lane East Hartford, Conn 06108
1	Prof George Mellor Dept Aerospace & Mechn Sci Engrg Quad Princeton Univ Princeton, N.J. 08540
1	Prof A.F. Mills Univ of Calif, Los Angeles Dept Engrg Los Angeles, Calif 90024
1	Prof Mark Morkovin Ill Institute of Technology Aerospace & Mech Engrg Dept Chicago, Ill
1	Dr. Hal L. Moses Project Engr Corning Glass Works 3800 Electronics Drive Raleigh, N.C. 27604
1	Mr. John Murphy Mail Stop 227-8 NASA, Ames Research Center Moffett Field, Calif 94035
1	Dr. John P. Nash Aerospace Sci Lab Dept 72-14 Zone 403 Lockheed-Georgia Co Marietta, Ga. 30060
1	Prof Victor Nee Dept Mech Engrg Univ of Notre Dame Notre Dame, Indiana 46556
1	Dr. H.J. Nielsen Nielsen Engrg & Research Co 2460 Park Blvd P.O. Box 11228 Palo Alto, Calif 94306

Copies	
1	Dr. Elrich Plate Fluid Dynamics & Diffusion Lab College of Engrg Colorado State Univ Fort Collins, Colorado
1	Mr. Ted Reyhner c/o Bert Welliver Prop. Research Unit Boeing Aircraft P.O. Box 707 Renton, Washington
1	Prof W.C. Reynolds Mech Engrg Dept Thermosciences Div Stanford Univ Stanford, Calif 94305
1	Mr. W.C. Rose Mail Stop 227-8 NASA, Ames Research Center Moffett Field, Calif 94035
1	Dr. M. Rubesin Mail Stop 230-1 NASA, Ames Research Center Moffett Field, Calif 94035
1	Prof V.A. Sandborn Colorado State Univ Fort Collins, Colorado 80521
1	Dr. G. Sovran Engrg Development Dept Research Labs General Motors Techn Center 12 Mile & Mound Rds Warren, Michigan 48090
1	Dr. Joseph Sternberg Martin Marietta Corp Aerospace Headquarters Friendship International Airport, Baltimore, Md 21240
1	Prof Itiro Tani c/o Dept of Mechanics JHU (Homewood Campus) Baltimore, Md 21218
1	Prof H. Tennekes Aerospace Engrg Dept 153E Hammond Bldg Penn State Univ Univ Park, Pa 16802

Copies	
1	Dr. Earl M. Uram Assistant Dean Graduate School of Engrg Univ of Bridgeport Bridgeport, Conn 06602
1	Dr. W.W. Willmarth Dept Aerospace Engrg Univ of Michigan Ann Arbor, Michigan 48104
1	Capt J.D. Young AFWL (WLDE-3) Kirtland Air Force Base New Mexico 87117
1	Prof V.W. Goldschmidt Dept Mech Eng Purdue Univ Lafayette, Ind. 47907
1	Dr. J.J. Cornish III Aerospace Sciences Lab Dept 72-14 Zone 403 Lockheed-Georgia Co Marietta, Ga. 30060

UNCLASSIFIED

Security Classification

DOCUMENT CONTROL DATA - R & D

(Security classification of title, body of abstract and indexing annotation must be entered when the overall report is classified)

1. ORIGINATING ACTIVITY *(Corporate author)* Naval Ship Research and Development Center Washington, D.C. 20007	2a. REPORT SECURITY CLASSIFICATION UNCLASSIFIED 2b. GROUP

3. REPORT TITLE

INTEGRAL METHODS FOR TURBULENT BOUNDARY LAYERS IN PRESSURE GRADIENTS

4. DESCRIPTIVE NOTES *(Type of report and inclusive dates)*

Final Report

5. AUTHOR(S) *(First name, middle initial, last name)*

Paul S. Granville

6. REPORT DATE	7a. TOTAL NO. OF PAGES	7b. NO. OF REFS
April 1970	55	33

8a. CONTRACT OR GRANT NO.	9a. ORIGINATOR'S REPORT NUMBER(S)
b. PROJECT NO. UR 109 01 03	3308
c.	9b. OTHER REPORT NO(S) *(Any other numbers that may be assigned this report)*
d.	AD 707 074

10. DISTRIBUTION STATEMENT

This document has been approved for public release and sale; its distribution is unlimited.

11. SUPPLEMENTARY NOTES	12. SPONSORING MILITARY ACTIVITY Naval Ordnance Systems Command Washington, D.C. 20360

13. ABSTRACT

Shape parameter differential equations are developed for turbulent boundary layers in pressure gradients incorporating two-parameter velocity profiles. Energy and entrainment methods are included. Shear stress factors are explicitly developed for equilibrium and quasi-equilibrium conditions.

14 KEY WORDS	LINK A		LINK B		LINK C	
	ROLE	WT	ROLE	WT	ROLE	WT
Boundary layer						
Pressure gradient						
Velocity profile						